Technical Memorandum 26

A simple computer model for terrestrial and solar radiation transfer

I.M. Vardavas and L.M. Cannon

Supervising Scientist for the Alligator Rivers Region

Supervising Scientist for the

Alligator Rivers Region

TECHNICAL MEMORANDUM 26

A SIMPLE COMPUTER MODEL FOR TERRESTRIAL AND SOLAR RADIATION TRANSFER

Ilias M. Vardavas and Lisa M. Cannon

Australian Government Publishing Service

Canberra 1989

ISSN 0810-9532
ISBN 0 644 09133 9

Supervising Scientist for the Alligator Rivers Region
P.O. Box 387, Bondi Junction
N.S.W. 2022, Australia

This Technical Memorandum was prepared by:

Ilias M. Vardavas and Lisa M. Cannon

of the Office of the Supervising Scientist
for the Alligator Rivers Region

The Supervising Scientist for the Alligator Rivers Region manages the Alligator Rivers Region Research Institute, which conducts, co-ordinates and integrates research relating to the effects on the environment of uranium mining in the Alligator Rivers Region. Research findings of projects carried out under contract to the Supervising Scientist or undertaken by the Supervising Scientist's own staff may be published in the Research Report or Technical Memorandum series. Views expressed by authors do not necessarily reflect the views and policies of the Supervising Scientist, the Commonwealth Government or any collaborating organisation.

Printed in Australia by Alken Press Pty. Ltd. – Smithfield

CONTENTS

FIGURES

ABSTRACT

Ilias M. Vardavas & Lisa M. Cannon (1989). A simple computer model for terrestrial and solar radiation transfer. Technical Memorandum 26, Supervising Scientist for the Alligator Rivers Region.

A simple radiative-convective atmospheric model is presented for rapidly computing the solar and terrestrial fluxes at the top of the atmosphere and at the ground. The model parameters are measurable meteorological quantities with water vapour playing a key role in the determination of the ratio of infrared flux emitted by a water surface to the absorbed solar flux; this infrared fraction is important in Heat Balance evaporation models. The model and its computer programme can be used to examine, for example, the response of the global mean surface temperature to changes in CO_2, cloud cover and solar-constant.

EXPLANATORY NOTES

Pressure Levels

p_g = ground pressure
p_c = cloud top pressure
p_{cb} = cloud base pressure

Atmosphere IR Optical Depths and Transmissivities

$\tau_g = \tau(0,p_g)$ = total optical depth
$\tau_c = \tau(0,p_c)$ = above cloud optical depth
$\tau_{cb} = \tau(p_{cb},p_g)$ = below cloud optical depth

$t_g = \exp(-\tau_g)$ = total transmissivity
$t_c = \exp(-\tau_c)$ = above cloud transmissivity
$t_{cb} = \exp(-\tau_{cb})$ = below cloud transmissivity

$t_1 = \exp(-\tau(p,0))$ = transmissivity between pressure level p and top of atmosphere
$t_2 = \exp(-\tau(p,p_g))$ = transmissivity between pressure level p and ground
$t_3 = \exp(-\tau(p,p_{cb}))$ = transmissivity between pressure level p and cloud base ($p>p_{cb}$)
$t_4 = \exp(-\tau(p,p_c))$ = transmissivity between p and cloud top ($p < p_c$)

1 INTRODUCTION

Recently, Vardavas & Carver (1984*a,b*) developed a one dimentional (1-D) radiative-convective modelling technique for rapidly computing the mean vertical atmospheric temperature profile. They presented parameterizations for both solar (~ 0.1-5.0 μm) and terrestrial (greater than about 5 μm) radiation transfer. The infrared, visible and ultraviolet regions were divided into fine spectral intervals within which atmospheric molecules of water vapour (H_2O), carbon dioxide (CO_2), ozone (O_3), methane (CH_4) and ammonia (NH_3) have important absorption bands.

This fine spectral radiation transfer was devised in order to model climatic change due to spectral variations in the solar flux and changes in the terrestrial surface albedo (or reflectivity). The model has been used to examine the response of the earth's global mean vertical temperature to changes in atmospheric composition (e.g. changes in CO_2 and CH_4), cloud cover and solar-constant (Vardavas & Carver 1985), and to solar cycle uv flux variations (Vardavas 1987*a*).

In the present work, a simpler version (SV) of the above more complex model (CV) is presented. It is based on simple expressions for the total absorption of infrared, visible and ultraviolet radiation by the atmospheric molecules. This allows the atmosphere to be represented as layers having simple transmission coefficients (or transmissivities) which depend on the amount of absorbing molecules in each layer.

The present simple model can be used to compute rapidly solar and terrestrial radiation fluxes at the top of the atmosphere and at the ground using measurable meteorological quantities as model input parameters. It can be easily included in Heat Balance models to compute the net all-wave flux absorbed by a water surface (Vardavas 1987*b*) while the mean global surface temperature can be readily computed from flux balance between net all-wave incoming and outgoing radiation fluxes at the top of the atmosphere. The present model can thus be used to examine the effects of climatic change due, for example, to changes in atmospheric CO_2, cloud cover and solar-constant.

The atmospheric model is described in Section 2. The 1-D vertical temperature structure consists of a troposphere with a temperature structure determined by a specified adiabatic lapse rate while the lower stratosphere is taken to be isothermal with a temperature fixed at the tropopause temperature. In Section 3 the evaluation of the terrestrial flux is described both for a clear and cloudy sky. Expressions are derived for computing the net infrared flux at the ground and at the top of the atmosphere. In Section 4 the solar radiation transfer is described and an expression is derived for the planetary albedo which determines the net incoming solar flux at the top of the atmosphere and the net solar flux incident on the ground. Model flux and temperature computations using the present SV model are compared with those of the complex CV model in Section 5. The computer programme and its documentation are given in Section 6. Two sample computer runs are included; one computes the mean global surface temperature, the other computes the radiation fluxes at the top of the atmosphere and at the ground for a specified atmospheric temperature profile.

2 ATMOSPHERIC MODEL

2.1 Radiative equilibrium

In the present 1-D radiative-convective model, flux balance at the top of the atmosphere is used to determine the earth's mean global surface temperature, T_g. The earth is taken to be in radiative equilibrium and so the net flux at the top of the atmosphere is set equal to zero (see Fig. 1):

$$\bar{F}_{ir}^{\uparrow}(\infty) - \bar{F}_{o}^{\downarrow}(\infty) = 0 \qquad (1)$$

where $\bar{F}_{ir}^{\uparrow}(\infty)$ is the net outgoing terrestrial infrared flux (Wm^{-2}) and $\bar{F}_{o}^{\downarrow}(\infty)$ is the net incoming solar flux at the top of atmosphere. The terrestrial flux is a strong function of the vertical atmospheric temperature structure and the atmospheric infrared opacity. The surface temperature of the earth, T_g, is obtained iteratively from the flux balance equation. The solar flux absorbed by the atmosphere is weakly dependent on the atmospheric temperature profile but is strongly dependent on the atmospheric gases.

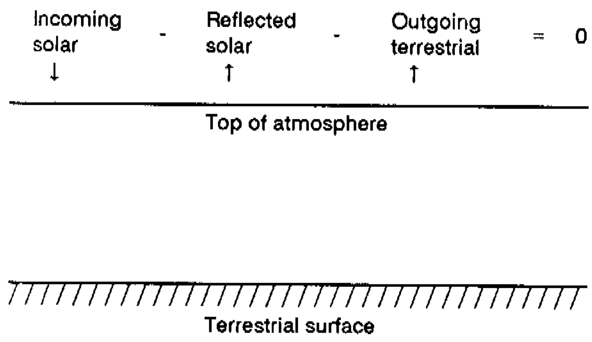

Figure 1. Flux balance at the top of the atmosphere

2.2 Radiation fields

Incident solar radiation is either absorbed by the surface-atmosphere system or is reflected back to space. The absorbed solar radiation is re-emitted by the surface-atmosphere as terrestrial radiation.

The atmospheric absorption and emission of the solar and terrestrial radiation fields can be treated separately because the flux emitted by the sun consists mainly of short-wave radiation (~ 0.1-5.0 μm) while the flux emitted by the earth consists of infrared radiation (> 5 μm). Idealized spectral distributions of the two radiation fields are shown in Fig. 2 (Note the difference in units between solar and terrestrial fields). The distributions were generated by Planck functions with T = 5770 K for the sun and T = 252 K for the earth, corresponding to the effective black body temperatures of the two bodies.

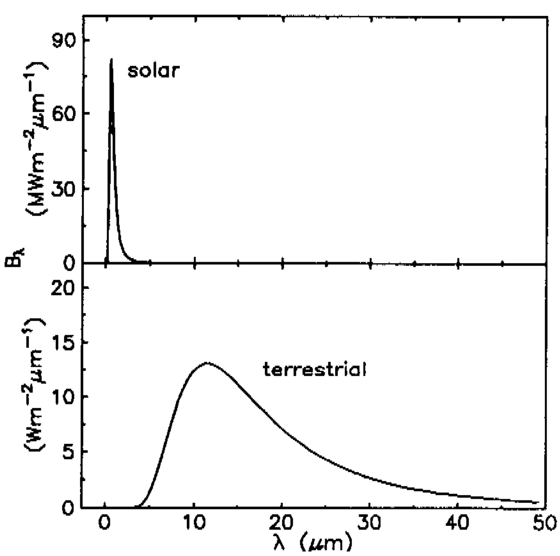

Figure 2. The spectral distributions of solar and terrestrial radiation fields

2.3 Greenhouse effect of the atmosphere

The atmosphere is an envelope of gas and clouds which surrounds the earth and which greatly affects the earth's temperature. Solar radiation incident on the surface is reflected, absorbed and re-emitted. Without an atmosphere all of the re-emitted (or terrestrial) radiation would escape to space. However, the presence of an atmosphere results in part of the outgoing terrestrial radiation being absorbed, scattered and re-emitted by the atmosphere back towards the earth. This reduces the total terrestrial flux escaping from the earth and significantly increases the earth's surface temperature, T_g.

2.4 Temperature profile

Differential absorption of energy by gas molecules within each atmospheric layer results in a vertical atmospheric temperature profile, as illustrated by the U.S. Standard Atmosphere mean vertical temperature profile shown in Fig. 3.

The heated earth emits radiation which is transmitted to the atmosphere by convective and radiative interactions. In the troposphere (convection dominated lower atmosphere) the average temperature decreases with altitude from the surface at a rate called the adiabatic lapse rate, defined by:

$$\Gamma = -dT/dz \tag{2}$$

with Γ in units of K km^{-1} and z in km.

The stratosphere (radiation dominated middle atmosphere) is associated with the presence of ozone. Ozone strongly absorbs incoming ultraviolet solar radiation which heats the atmosphere and results in a gradual increase in temperature with altitude, with a peak at about 50 km. In the model, the temperature of the stratosphere is assumed to be constant at the tropopause level since the lower stratosphere is essentially isothermal (see Fig. 3) and because the pressure of the atmosphere decreases rapidly with altitude. The model temperature profile is thus taken to be:

$$T(p) = \begin{cases} T_g - \Gamma z(p) & p_T \le p \le p_g \\ T(p_T) & 0 \le p \le p_T \end{cases} \tag{3}$$

where p_T is the tropopause pressure and z(p) is the altitude at pressure p.

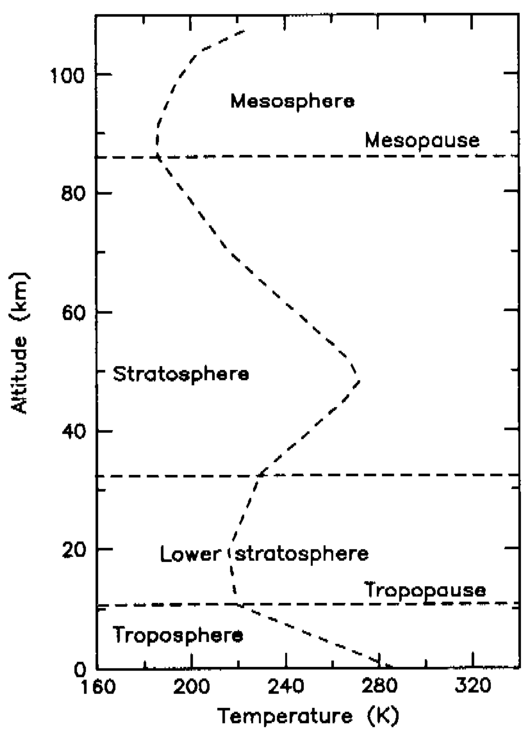

Figure 3. Vertical atmospheric temperature profile according to US Standard Atmosphere

2.5 Pressure profile

Since the vertical motions of the average atmosphere are generally very small, the atmosphere is assumed to be in hydrostatic equilibrium. This means that each infinitesimal layer of unit cross section can be described by:

$$dp = -g\rho dz \tag{4}$$

where ρ is the atmospheric density, g is the gravitational constant and dp is the upward pressure force that is balanced by the downward force of the gas weight. Using the assumed temperature structure, the hydrostatic equilibrium equation and the ideal gas law, the altitude can be expressed as a function of pressure. The ideal gas law can be written as:

$$\rho = p\bar{M}/RT \tag{5}$$

where $\bar{M}$ is the mean molecular weight, R is the universal gas constant and T is the temperature. Substituting for ρ the hydrostatic equilibrium equation becomes:

$$dp/p = -(g\bar{M}/RT)dz \tag{6}$$

On using the model temperature profile and integrating, the altitude-pressure profile becomes:

$$z(p) = \begin{cases} T_g \left[1 - (p/p_g)^{\alpha}\right] /\Gamma & \text{for } p_T \leq p \leq p_g \\ z(p_T) - \alpha T \ln(p/p_T)/\Gamma & \text{for } 0 \leq p \leq p_T \end{cases} \tag{7}$$

with $\alpha = \Gamma R/g\bar{M}$.

A fixed pressure grid is chosen to divide the atmosphere into levels and this allows T(p) to be readily computed given T_g and Γ.

3 TERRESTRIAL RADIATION

3.1 Emissivity

Throughout the surface-atmosphere system radiation is being absorbed and re-emitted. Absorbing radiation increases the kinetic energy of the particles, which at equilibrium is released as infrared radiation. The integrated wavelength flux emitted by a perfectly absorbing gas (or black body) is equal to σT^4, where T is the equilibrium temperature of the body of particles and $\sigma = 5.67 \times 10^{-8}$ $Wm^{-2}K^{-4}$ is the Stefan-Boltzman constant. For a non-perfectly absorbing gas or imperfect black body the emitted flux integrated over all wavelengths can be written as $\varepsilon\sigma T^4$, where ε is the emissivity of the body whose value ranges from 0 to 1.

The emitted flux is proportional to T^4 and thus a small change in temperature produces a large change in flux. The layers of gas in the dense lower atmosphere, the ground and low clouds essentially behave as black bodies and so $\varepsilon \simeq 1$ while the emissivity of cirrus or high clouds can be as low as 0.3. Local thermodynamic equilibrium conditions probably extend upto about the mesopause (e.g. Houghton 1979, p. 62).

3.2 Optical depth

Although a body may emit a flux F at an altitude $z(p_1)$, only a fraction, t, of F will reach $z(p_2)$ because of absorption in the layer between p_1 and p_2. This fraction is called the transmissivity of the gas layer between $z(p_1)$ and $z(p_2)$. The transmissivity can be written in terms of an 'atmospheric optical depth', τ (see Fig. 4). If the atmospheric optical depth (or opacity) is large, then the transmissivity is low. The transmissivity between $z(p_1)$ and $z(p_2)$ is defined by:

$$t = \exp(-\tau) \tag{8}$$

where $\tau = \tau(p_1,p_2)$ is the atmospheric optical depth between $z(p_1)$ and $z(p_2)$.

The wavelength integrated optical depth, τ, is dependent on the atmospheric absorber amount, pressure and temperature. The atmospheric absorber amount, W, for each absorber, a, is the number of grams of absorber gas per unit area (cm^2) between altitudes $z(p_1)$ and $z(p_2)$ and is given by:

$$W_a(p1,p2) = \int_{z1}^{z2} \rho_a dz \quad (9)$$

This can be expressed in terms of the mixing ratio which is given by:

$$\eta_a = \rho_a/\rho = p_a M_a/pM \quad (10)$$

where ρ_a, p_a, M_a are the density, pressure and molecular weight of the absorber and ρ, p, M those of air.

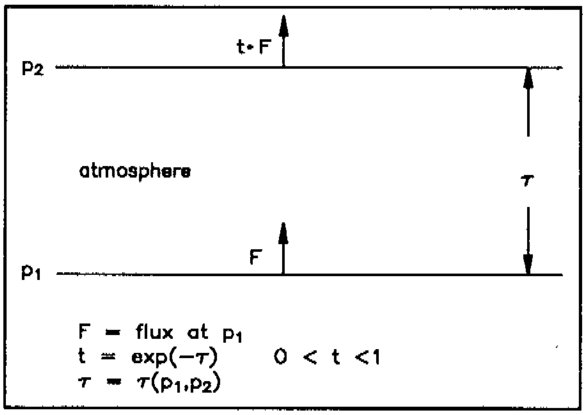

Figure 4. Flux transmission through an atmosphere layer between p_1 and p_2

Substituting $dp/g = -\rho dz$ and η_a in equation (9), the absorber amount becomes:

$$W_a(p1,p2) = -\int_{p1}^{p2} (\eta_a/g)dp, \qquad p1 > p2 \quad (11)$$

Although the main components of air are nitrogen, oxygen and argon, the most important absorbers are the trace constituents H_2O, CH_4, CO_2 and O_3 which strongly affect the atmospheric infrared transmission.

Water vapour decreases with altitude and this can be parameterized by:

$$\eta_{H2O} = \eta_{H2Og} \left(\frac{p}{p_g}\right)^{\beta} \quad (12)$$

where η_g refers to the surface mixing ratio at p_g.

Substituting equation (12) into (11) the water vapour absorber amount becomes:

$$W_{H2O}\ (p_1,p_2) = \eta_{H2Og}[p_1{}^{1+\beta} - p_2{}^{1+\beta}] \ / \ [(1 + \beta)gp_g{}^{\beta}] \quad (13)$$

where $p_1 > p_2$.

The total water vapour amount, $W^*_{H2O} = W_{H2O}(0,p_g)$, is then:

$$W^*_{H2O} = \eta_{H2Og}\ p_g \ / \ (1 + \beta)g \quad (14)$$

Therefore the water vapour absorber amount between $z(p_1)$ and $z(p_2)$ in terms of W^*_{H2O} is:

$$W_{H2O}(p_1,p_2) = W^*_{H2O}\ [(p_1/p_g)^{1+\beta} - (p_2/p_g)^{1+\beta}] \quad (15)$$

for $p_1 > p_2$.

A value of β is needed in terms of meteorological data.

From equation (14):

$$\beta = \eta_{H2Og}p_g \ / \ gW^*_{H2O} - 1 \quad (16)$$

Now since:

$$p_{H2O} = r_H \; e_s(T) \tag{17}$$

where r_H is the relative humidity (expressed as a fraction) and $e_s(T)$ is the saturation water vapour pressure (mbar) at temperature T:

$$p_{H2Og} = r_{Hg} \; e_s(T_g) \tag{18}$$

and from equation (10):

$$\eta_{H2Og} = p_{H2Og} \; M_{H2O}/p_g \; M \tag{19}$$

Substituting the last two equations into (16) gives:

$$\beta = 0.634 \; r_{Hg} \; e_s(T_g) \; / \; W^*_{H2O} - 1 \tag{20}$$

where $M_{H2O}/M = 0.62$, $g = 980.665$ cms^{-2}, W^*_{H2O} is a measurable meteorological quantity representing the total vertical water vapour amount (g cm^{-2}) and e_s in mbar is the saturation water vapour pressure at T given by:

$$\ln e_s = a_1 - a_2 \; / \; T + a_3 \ln T \tag{21}$$

where $a_1 = 58.1717$, $a_2 = 6938.67$ and $a_3 = -5.5189$ for $T > 273$ K.

For CO_2 and CH_4, η_a can be taken to be a constant. Integrating equation (11) for CH_4 and CO_2 the absorber amounts are:

$$W_{CO2}(p_1,p_2) = W^*_{CO2} \; (p_1 - p_2)/p_g \tag{23}$$

and

$$W_{CH4}(p_1,p_2) = W^*_{CH4} \; (p_1 - p_2)/p_g \quad \text{for } p_1 > p_2 \tag{24}$$

The ozone mixing ratio peaks within the stratosphere and the amount above level z (km) is computed from the expression of Green (1964):

$$W_{O3}(0,p) = W^*_{O3} \; G(z(p)) \tag{25}$$

$$\text{with} \quad G(z) = [1 + \exp(-b/c)] \; / \; [1 + \exp((z-b)/c)] \tag{26}$$

where for a mid-latitude ozone distribution b = 20 km and c = 5 km are representative values (see Lacis & Hansen 1974).

The ozone absorber amount between two altitudes $z(p_1)$ and $z(p_2)$ is:

$$W_{O3}(p_1,p_2) = W_{O3}(0,p_1) - W_{O3}(0,p_2) \quad \text{for } p_1 > p_2 \tag{27}$$

Substituting equation (25) into (27) gives:

$$W_{O3}(p_1,p_2) = W^*_{O3} \; [G(z(p_1)) - G(z(p_2))] \tag{28}$$

In Vardavas & Carver (1984*b*) the atmospheric infrared spectrum was divided into 22 broad intervals which have important water vapour, carbon dioxide, ozone and methane absorption bands. The flux was then computed at each atmospheric level for each spectral interval. The spectral flux was then summed to obtain the integrated flux at each atmospheric level.

In this work we are interested in computing the wavelength integrated flux at the top and at the base of the atmosphere. Since the atmospheric radiation field is primarily determined by the surface temperature T_g, it is characterised by a Planck function with a temperature in the vicinity of 200-300 K. In order to assign a wavelength averaged optical depth to the atmospheric layers we thus need to average the wavelength dependent optical depth weighted by the spectral distribution of the terrestrial radiation field and so we use the Planck mean optical depth to determine the transfer of integrated terrestrial radiation flux.

The Planck mean infrared optical depth τ of the whole atmosphere can be expressed as:

$$\tau = - \ln \bar{t} \tag{29}$$

$$\text{with} \quad \bar{t} = \int_0^\infty B_\lambda(T) t_\lambda d\lambda \;/\; \sigma T^4 \quad \simeq \sum_i \beta_i t_i \tag{30}$$

where $\beta_i(T) = \bar{B}_i(T)\ \Delta\lambda_i/\sigma T^4$, $\bar{B}_i$ is the mean value of the Planck function within spectral interval $\Delta\lambda_i$ and t_i is the associated mean transmission. The interval of integration extends from about 5 μm to infinity for T $\approx$ 300 K. Following the CV model of Vardavas & Carver (1984*b*), the interval of integration was divided into 22 sub-intervals which have important water vapour, carbon dioxide, ozone and methane infrared absorption bands. The β_i were found to be weakly temperature-dependent for the range 200-300 K and it was found that a useful simplification is to set $\beta_i(T) = \beta_i(T_*)$ with $T_* = 288$ K and then introduce a simple temperature correction to the optical depth τ via:

$$c(T_g) = -0.0045T_g + 2.3 \qquad \text{with } c(288) = 1.0 \tag{31}$$

This correction factor allows for the increase in the atmospheric mean optical depth with decreasing surface temperature. As the surface temperature decreases the peak in the Planck function, which describes the spectral flux emitted by the surface, moves to a higher wavelength and hence the relative contribution of the almost opaque water vapour bands beyond 20 μm increases (see Fig. 5).

Using equations (15), (23), (24) and (28), the Planck mean optical depth for each absorber amount W (gm cm^{-2}) can be readily evaluated from the following expressions based on the work of Vardavas & Carver (1984*b*):

$$\tau_{H2O}(p_1,p_2) = 0.63\ (W_{H2O})^{0.52} \quad \text{for } 0 \le W_{H2O} \le 10$$

$$\tau_{CO2}(p_1,p_2) = 0.14\ (W_{CO2})^{0.22} \quad \text{for } 0 \le W_{CO2} \le 10$$

$$\tau_{O3}(p_1,p_2) = 2.51\ (W_{O3})^{0.62} \quad \text{for } 0 \le W_{O3} \le 2.10^{-3}$$

and

$$\tau_{CH4}(p_1,p_2) = 2.51\ (W_{CH4})^{0.75} \quad \text{for } 0 \le W \le 10^{-2} \tag{32}$$

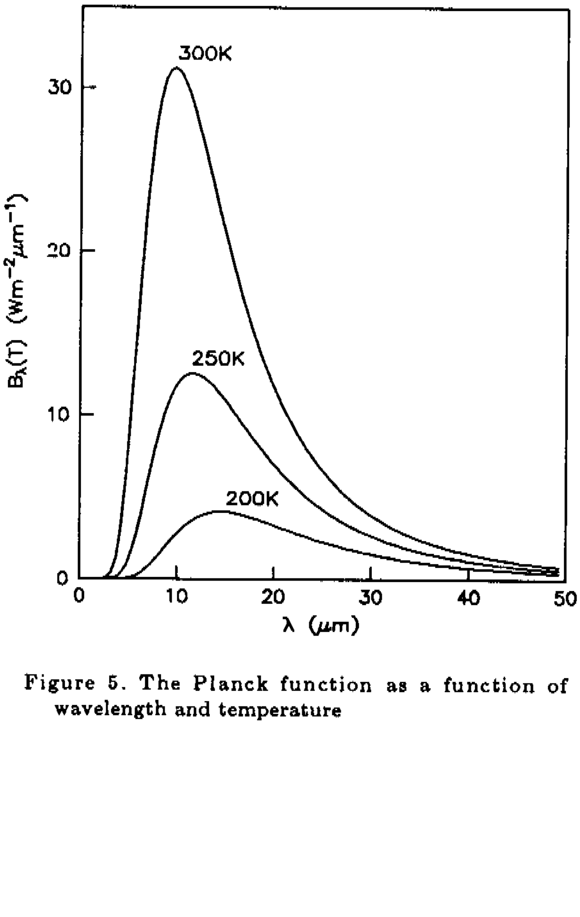

Figure 5. The Planck function as a function of wavelength and temperature

The atmospheric optical depth between $z(p_1)$ and $z(p_2)$ can then be expressed as:

$$\tau(p_1,p_2) = 1.66c(T_g)\,(\tau_{H2O}(p_1,p_2) + \tau_{O3}(p_1,p_2) + \tau_{CH4}(p_1,p_2) + \tau_{CO2}(p_1,p_2)) \tag{33}$$

where 1.66 is a standard diffusivity factor introduced to allow for non-vertical radiation transfer.

Note that the expressions in equation (32) are strictly valid only for the present total atmospheric pressure.

3.3 Clear sky fluxes

Net outgoing terrestrial flux

The net outgoing terrestrial flux consists of surface and atmospheric radiation. The surface emission is $\varepsilon_g \sigma T_g^4$, where ε_g is the emissivity and T_g is the temperature of the ground (see Fig. 6). However, only $t_g \varepsilon_g \sigma T_g^4$ reaches the top of the atmosphere where $t_g = \exp(-\tau_g)$ is the total atmospheric transmissivity, $\tau_g = \tau(0,p_g)$ and p_g is surface pressure.

The atmosphere can be divided into pressure or optical depth layers each emitting infrared radiation according to its average gas temperature. The radiation emitted from these layers can reach the top of the atmosphere either directly or reflected from the surface. Each atmospheric layer at temperature T emits a flux equal to σT^4, but only $t_1 \sigma T^4$ reaches the top of the atmosphere directly, where $t_1 = \exp(-\tau(0,p))$ is the transmissivity between the layer at z(p) and the top of the atmosphere z(p = 0). Summing over all the atmospheric layers (p = 0 to p = p_g), the flux reaching the top of the atmosphere directly is given by:

$$\int_0^{\tau_g} t_1 \sigma T^4 d\tau, \quad t_1 = \exp(-\tau(p,0)) \text{ and } \tau_g = \tau(0,p_g)$$

Each gas layer also emits σT^4 in the direction of the earth. This is first reduced by $t_2 = \exp(-\tau(p,p_g))$. Then at the surface a fraction ε_g is absorbed and a fraction $1 - \varepsilon_g$ is reflected. Finally only t_g of the reflected flux reaches the top of the atmosphere. Therefore the flux reaching the top of the atmosphere via the earth's surface is $t_g\,(1 - \varepsilon_g)\,t_2\,\sigma T^4$. Summing over all of the gas layers from p = 0 to p = p_g, the flux reaching the top of the atmosphere indirectly is equal to:

$$(1 - \epsilon_g)t_g \int_0^{\tau_g} t_2 \sigma T^4 d\tau, \quad t_2 = \exp(-\tau(p,p_g))$$

The net outgoing terrestrial flux under a clear sky at the top of the atmosphere is given by the sum of the above components (see Fig. 6).

$$\overline{F}_s^{\uparrow}(\infty) = t_g \epsilon_g \sigma T_g^4 + \int_0^{\tau_g} t_1 \sigma T^4 d\tau + (1-\epsilon_g)\int_0^{\tau_g} t_g t_2 \sigma T^4 d\tau \tag{34}$$

The net flux can be re-written as:

$$\overline{F}_s^{\uparrow}(\infty) = \overline{t}_s \varepsilon_g \sigma T_g^4 \quad (35)$$

where $\overline{t}_s$ is an effective atmospheric transmissivity for a clear sky and is given by:

$$\overline{t}_s = t_g + \frac{1}{\epsilon_g} \int_0^{\tau_g} \left(\frac{T}{T_g}\right)^4 t_1 d\tau$$

$$+ \frac{(1-\epsilon_g)}{\epsilon_g} t_g \int_0^{\tau_g} \left(\frac{T}{T_g}\right)^4 t_2 d\tau \quad (36)$$

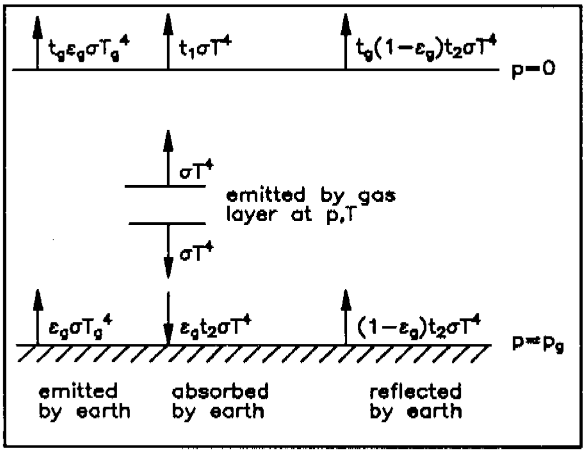

Figure 6. The clear sky transmission of terrestrial flux emitted by the ground and each atmospheric layer

Net upward flux at the surface

Understanding the derivation of $\overline{F}_s^{\uparrow}(\infty)$, it is easy to derive the equations for the net upward terrestrial flux at the surface, $\overline{F}_s^{\uparrow}(0)$, a flux that is important in solar evaporation models.

At the surface, the net upward terrestrial flux for a clear sky atmosphere may be evaluated from:

$$\overline{F}_s^{\uparrow}(0) = \overline{\varepsilon}_s \sigma T_g^4 \quad (37)$$

where $\overline{\varepsilon}_s$ represents an effective ground emissivity for a clear sky atmosphere and is given by:

$$\overline{\epsilon}_s = \epsilon_g - \epsilon_g \int_0^{\tau_g} \left(\frac{T}{T_g}\right)^4 t_2 d\tau + (1-\epsilon_g) \int_0^{\tau_g} \left(\frac{T}{T_g}\right)^4 t_2 d\tau \quad (38)$$

The first term in equation (38) is the ground emittance, the second term is the atmospheric flux absorbed by the surface, while the third is the atmospheric flux reflected by the surface (see Fig. 6).

3.4 Cloud cover

Clouds cover approximately 50% of the earth and significantly affect the surface temperature by reflecting to space a fraction of the incident solar radiation. Clouds also act as thermal insulators by absorbing the upward terrestrial flux and re-radiating it back towards the ground.

The total cloud cover fraction A_c can be estimated from day length d (h) and sunshine hours from:

$$A_c = 1 - s/d \quad (39)$$

In the present model the total cloud cover, which includes the effect of overlapping cloud layers, is divided into three non-overlapping components which are contributed by low clouds, middle clouds and high clouds (see Fig. 7). The contribution A_{ci} of each cloud type to the total cloud cover is evaluated from:

$$A_{ci} = f_i e_i A_c / \sum_i f_i e_i \qquad (40)$$

where f_i is a cloud frequency of occurrence weight and e_i is a cloud extent weight given by:

$$f_i = n_i / \sum_i n_i \quad \text{and} \quad e_i = A'_{ci} / \sum_i A'_{ci} \qquad (41)$$

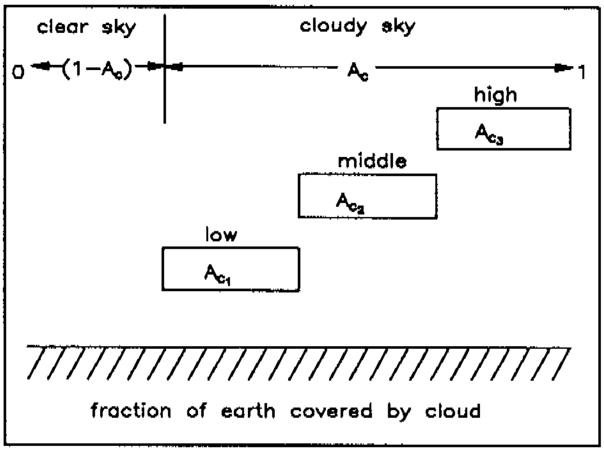

Figure 7. A sky described by a clear sky and cloudy sky fraction, where the cloudy sky fraction comprises three non-overlapping layers

with n_i the frequency of occurrence of cloud type i and A'_{ci} is the observed average fractional cloud cover. The total cloud cover is then given by:

$$A_c = \sum_i A_{ci} \qquad (42)$$

3.5 Cloudy sky fluxes

Net outgoing terrestrial flux

The net outgoing terrestrial flux for a cloudy sky comprises the atmospheric, cloud and surface emitted flux (See Fig. 8).

Cloud emitted flux reaching the top of the atmosphere equals $t_c\ \varepsilon_c \sigma T_c^4$, where t_c is the above cloud atmospheric transmissivity, ε_c is the cloud emissivity and T_c the temperature of the cloud top, where $t_c = \exp(-\tau(0,p_c))$ and p_c is the cloud top pressure.

From a gas layer situated above the cloud, the flux that reaches the top of the atmosphere equals $t_1 \sigma T^4$, where t_1 is the transmissivity between the layer at p and the top of the atmosphere. Summing over all the atmospheric layers above the cloud, the outgoing flux contributed by these atmospheric layers is given by:

$$\int_0^{\tau_c} t_1 \sigma T^4 d\tau, \quad t_1 = \exp(-\tau(p,0))$$

$$\text{and } \tau_c = \tau(0,p_c)$$

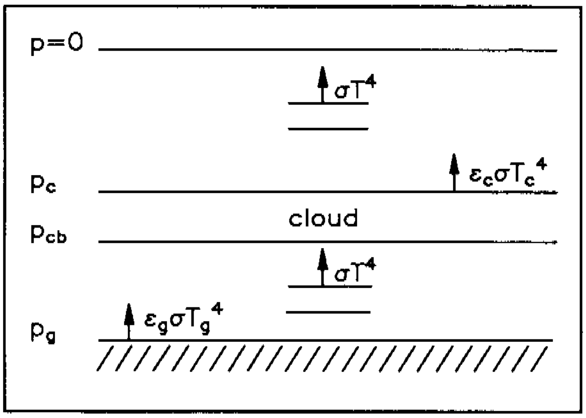

Figure 8. The four sources of outgoing terrestrial radiation for a cloudy sky are: the ground, the cloud and the atmospheric layers above and below the cloud

The flux emitted from a gas layer situated below the cloud, goes through three reductions. Firstly, by transmission through the atmosphere below the cloud layer it is reduced by a factor $t_3 = \exp(-\tau(p,p_{cb}))$, where p_{cb} is the cloud base pressure. Secondly, the flux passes through the cloud and is reduced by a factor $1 - \varepsilon_c$, where ε_c is the absorptivity (equal to the emissivity) of the cloud. Thirdly, by transmission through the atmosphere above the cloud layer it is reduced by a factor t_c. Therefore the flux reaching the top of the atmosphere from a gas layer situated below the cloud is equal to $\sigma T^4\ t_3\ (1 - \varepsilon_c)t_c$. Summing over all the layers below the cloud (from $p = p_g$ to $p = p_{cb}$), the contributed flux is:

$$(1 - \epsilon_c)t_c\int_0^{\tau_{cb}} t_3\sigma T^4 d\tau, \quad t_3 = \exp(-\tau(p,p_{cb})) \quad \text{and} \quad \tau_{cb} = \tau(p_{cb},p_g)$$

The surface emitted infrared flux $\varepsilon_g\sigma T_g^4$ reaching space is reduced by the atmosphere above and below the cloud and by the cloud itself. The flux reaching the top of the atmosphere from the ground is thus $t_{cb}\ (1 - \varepsilon_c)\ t_c\ \varepsilon_g\sigma T_g^4$, where $t_{cb} = \exp(-\tau_{cb})$.

The net outgoing flux under a cloudy sky, $\overline{F}_c^{\uparrow}(\infty)$, is thus given by the sum of the above components.

$$\overline{F}_c^{\uparrow}(\infty) = t_c\epsilon_c\sigma T_c^4 + \int_0^{\tau_c} t_1\sigma T^4 d\tau + (1 - \epsilon_c)\ t_c \int_0^{\tau_{cb}} t_3\sigma T^4 d\tau$$

$$+ t_{cb}\ (1 - \epsilon_c)\ t_c\ \epsilon_g\sigma T_g^4 \tag{43}$$

The net outgoing flux for a cloudy atmosphere at the top of the atmosphere can also be written as:

$$\overline{F}_c^{\uparrow}(\infty) = \overline{t}_c\ \varepsilon_c\sigma T_c^4 \tag{44}$$

with

$$\overline{t}_c = t_c + \frac{1}{\epsilon_c}\left(\frac{T_g}{T_c}\right)^4 \int_0^{\tau_c} t_1 \left(\frac{T}{T_g}\right)^4 d\tau + \frac{(1 - \epsilon_c)}{\epsilon_c}\ t_c \left(\frac{T_g}{T_c}\right)^4 \int_0^{\tau_{cb}} \left(\frac{T}{T_g}\right)^4 t_3\ d\tau$$

$$+ t_{cb}\ \frac{(1 - \epsilon_c)}{\epsilon_c}\ t_c\ \epsilon_g \left(\frac{T_g}{T_c}\right)^4 \tag{45}$$

The net outgoing terrestrial flux for the whole sky is the sum of clear sky and cloudy sky net outgoing fluxes weighted by the fractional cloud cover.

$$\overline{F}_{ir}^{\uparrow}(\infty) = (1 - A_c)\ \overline{F}_s^{\uparrow}(\infty) + \sum_i A_{ci}\ \overline{F}_c^{\uparrow}(\infty)_i \tag{46}$$

where $\overline{F}_c^{\uparrow}(\infty)_i$ is the net outgoing flux above cloud type i and $\overline{F}_s(\infty)$ is the net outgoing flux from the clear sky.

$\overline{F}_{ir}^{\uparrow}(\infty)$ can be written as:

$$\overline{F}_{ir}^{\uparrow}(\infty) = \overline{t}_f\sigma T_g^4 \tag{47}$$

where

$$\overline{t}_f = (1 - A_c)\overline{t}_s\varepsilon_g + \sum_i A_{ci}\, \overline{t}_{ci}\, \varepsilon_{ci}\, (T_{ci}/T_g)^4 \tag{48}$$

If we let $fr_i = A_{ci}/A_c$ then equation (46) can be written as:

$$\overline{F}_{ir}^{\uparrow}(\infty) = \sum_i fr_i\, \overline{F}_{ir}^{\uparrow}(\infty)_i \tag{49}$$

where

$$\overline{F}_{ir}^{\uparrow}(\infty)_i = (1 - A_c)\overline{F}_s^{\uparrow}(\infty) + A_c\, \overline{F}_c^{\uparrow}(\infty)_i \tag{50}$$

In evaluating the above integrals it is important to integrate in the correct direction.

Let F^+ be the total flux emitted from all layers of the atmosphere between levels z_1 and z_2 reaching p_2 and F^- be the flux emitted from all layers of the atmosphere between levels z_1 and z_2 reaching p_1. Then it is important to note that $F^+ \neq F^-$ because the density of the gas varies with altitude and so the flux reaching level p_1 is dominated by radiation emitted from the adjacent layers which do not have the same absorber amounts as layers adjacent to p_2.

Net upward flux at the surface

Below a cloud layer the net upward flux $\overline{F}_c^{\uparrow}(0)$ has three components: the surface emittance, the absorbed flux at the surface and the atmospheric flux reflected by the surface (see Fig. 9). The surface absorbs ε_g and reflects $(1-\varepsilon_g)$ of the incident flux which has three components. These comprise the flux from the atmosphere below the cloud layer, f_1, the flux from the cloud base, f_2, and the atmospheric flux from above the cloud layer, f_3 and are given by:

$$f1 = \int_0^{\tau_{cb}} t_2\sigma T^4 d\tau \qquad f2 = t_{cb}\,\sigma T_c^4 \quad \text{and} \quad f3 = t_{cb}(1 - \epsilon_c)\int_0^{\tau_c} t_4\,\sigma T^4\, d\tau \tag{51}$$

with $t_4 = \exp(-\tau(p,p_c))$.

The net upward flux at the surface below the cloud layer is then:

$$\overline{F}_c^{\uparrow}(0) = \varepsilon_g\,\sigma T_g^4 + (1 - \varepsilon_g)\,(f_1 + f_2 + f_3) - \varepsilon_g(f_1+f_2+f_3) \tag{52}$$

which can be re-written as:

$$\overline{F}_c^{\uparrow}(0) = \overline{\varepsilon}_c\,\sigma T_g^4 \tag{53}$$

where $\overline{\varepsilon}_c$ is the effective surface emissivity below the cloud given by:

$$\overline{\varepsilon}_c = \varepsilon_g + (1 - \varepsilon_g)\,(f_1 + f_2 + f_3)/\sigma T_g^4 - \varepsilon_g(f_1 + f_2 + f_3)\,/\sigma\, T_g^4 \tag{54}$$

For a number of different non-overlapping cloud types i we have:

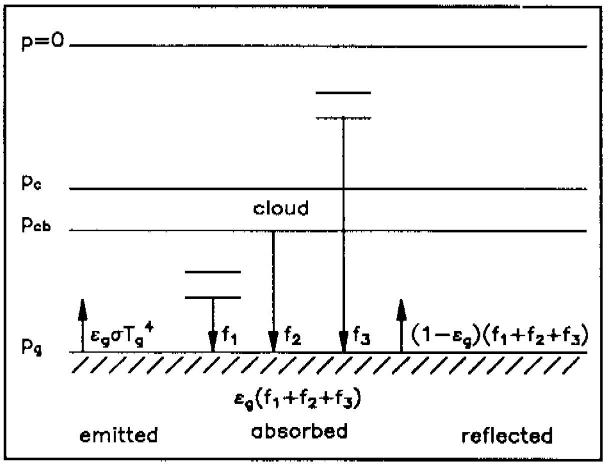

Figure 9. The emitted, absorbed and reflected components of terrestrial flux at the surface beneath a cloudy sky

$$A_c\bar{\varepsilon}_c = \sum_i A_{ci}\bar{\varepsilon}_{ci}. \tag{55}$$

The total net upward terrestrial flux at the ground is then:

$$\bar{F}_{ir}^{\uparrow}(0) = (1 - A_c)\bar{F}_s^{\uparrow}(0) + \sum_i A_{ci}\, \bar{F}_c^{\uparrow}(0)_i \tag{56}$$

where $\bar{F}_c^{\uparrow}(0)_i$ is the net upward flux at the surface below cloud type i and $\bar{F}_s^{\uparrow}(0)$ is the net upward flux for a clear sky at the surface.

In terms of the fraction $fr_i = A_{ci}/A_c$ equation (56) can be written as:

$$\bar{F}_{ir}^{\uparrow}(0) = \sum_i fr_i\, \bar{F}_{ir}^{\uparrow}(0)_i \tag{57}$$

where

$$\bar{F}_{ir}^{\uparrow}(0)_i = (1-A_c)\, \bar{F}_s^{\uparrow}(0) + A_c\, \bar{F}_c^{\uparrow}(0)_i \tag{58}$$

4 SOLAR RADIATION

4.1 Incoming flux

The mean daily incoming solar flux is given by:

$$F_{IN}^{\downarrow} = S_o\bar{\mu}\; d/r^2 \quad (Jm^{-2}\ day^{-1}) \tag{59}$$

Where S_o is the solar constant (1367 Wm^{-2}, Frohlich 1983), $\bar{\mu}$ is the daily mean cosine of the solar zenith angle, d is the daylength (s) and $1/r^2$ is a correction factor due to earth's elliptical orbit. The daylength is given by:

$$d = 8.64 \times 10^4\ H/\pi \quad (s) \tag{60}$$

The correction factor $1/r^2$ can be evaluated from:

$$r = (1 - e^2)/(1 + e \cos\nu) \tag{61}$$

which is the ratio of the magnitude of the radius vector of the earth's orbit to the mean distance between the earth and sun, where $e = 0.0167$ is the orbit eccentricity, ν is the obliquity of the sun given by $\nu = 78° - \lambda$ with $\sin\lambda = \sin\delta/\sin\delta_o$ where λ is its longitude, δ its declination and $\delta_o = 23.45°$.

The cosine of the solar zenith angle, μ, varies throughout the day. However, the mean daily solar zenith angle $\bar{\mu}$ is given by:

$$\bar{\mu} = A + B\ (\sin H)/H \tag{62}$$

where H is the hour angle given by:

$$\cos H = -\tan\phi\, \tan\delta \tag{63}$$

where ϕ is the latitude of a given location on earth, and

$$A = \sin\phi\, \sin\delta \tag{64}$$

$$B = \cos\phi\, \cos\delta \tag{65}$$

For seasonally and diurnally averaged conditions we can take a mean daylength of $d = \frac{1}{2}$ day, i.e. $H = \pi/2$, and $\delta = 0$ (at equinox) so that the mean solar zenith angle at latitude ϕ is given by:

$$\bar{\mu}(\phi) = 2 \cos \phi/\pi \tag{66}$$

We can then evaluate a global or latitudinal mean for the solar zenith angle by noting that the fraction of the spherical surface area contained within a latitudinal interval $d\phi$ is $\cos\phi d\phi$ so that the surface weighted mean is given by:

$$\bar{\mu} = \int_0^{\pi/2} \mu(\phi)\cos\phi d\phi \tag{67}$$

assuming the earth to be a perfect sphere. Thus $\bar{\mu}$ can be evaluated from:

$$\bar{\mu} = \frac{2}{\pi}\int_0^{\pi/2} \cos^2\phi d\phi \tag{68}$$

$$= 1/2$$

The mean global daily incoming solar flux can then be obtained from equation (59) by setting d = 1/2 day, $\bar{\mu}$ = 1/2 and r $\simeq$ 1 so that:

$$F_{IN}^{\downarrow} \simeq S_o/4 \quad (\mathrm{Wm}^{-2}) \tag{69}$$

In order to compute the global mean surface temperature the mean global daily net incoming solar flux is needed. This can be evaluated from:

$$\bar{F}_o^{\downarrow}(\infty) = (1 - R_p)F_{IN}^{\downarrow} = a\ F_{IN}^{\downarrow} \tag{70}$$

where R_p is the planetary albedo and a is the planetary absorptivity.

The absorptivity, a, can be written in terms of the clear sky planetary absorptivity, a_s, and cloudy sky absorptivity a_{ci} for a cloud type i covering a fraction A_{ci} of the sky:

$$a = (1-A_c)a_s + \sum_i A_{ci}\ a_{ci} \tag{71}$$

So that

$$\bar{F}_o^{\downarrow}(\infty) = F_{IN}^{\downarrow}\ [(1-A_c)a_s + \sum_i A_{ci}\ a_{ci}] \tag{72}$$

This can also be written in terms of the fraction, $fr_i = A_{ci}/A_c$, as:

$$\bar{F}_o^{\downarrow}(\infty) = \sum_i fr_i\ \bar{F}_o^{\downarrow}(\infty)_i$$

where

$$\bar{F}_o^{\downarrow}(\infty)_i = F_{IN}^{\downarrow}\ [(1-A_c)a_s + A_c\ a_{ci}] \tag{73}$$

4.2 Planetary albedo

The planetary albedo, R_p, is modelled by considering a four layer atmosphere (see Figs 10 and 11). At the top is an ozone layer which transmits only a fraction, t_{uv}, of the incoming solar flux, $S_o/4$, because of ultraviolet absorption between 0.2-0.35 μm corresponding to about 4.5% of the incoming solar radiation. If all uv is absorbed, then 95.5% of incoming solar radiation will be transmitted, which corresponds to t_{uv} having a minimum value of 0.955. The ozone layer also absorbs in the visible (0.45-0.85 μm) corresponding to 45% of

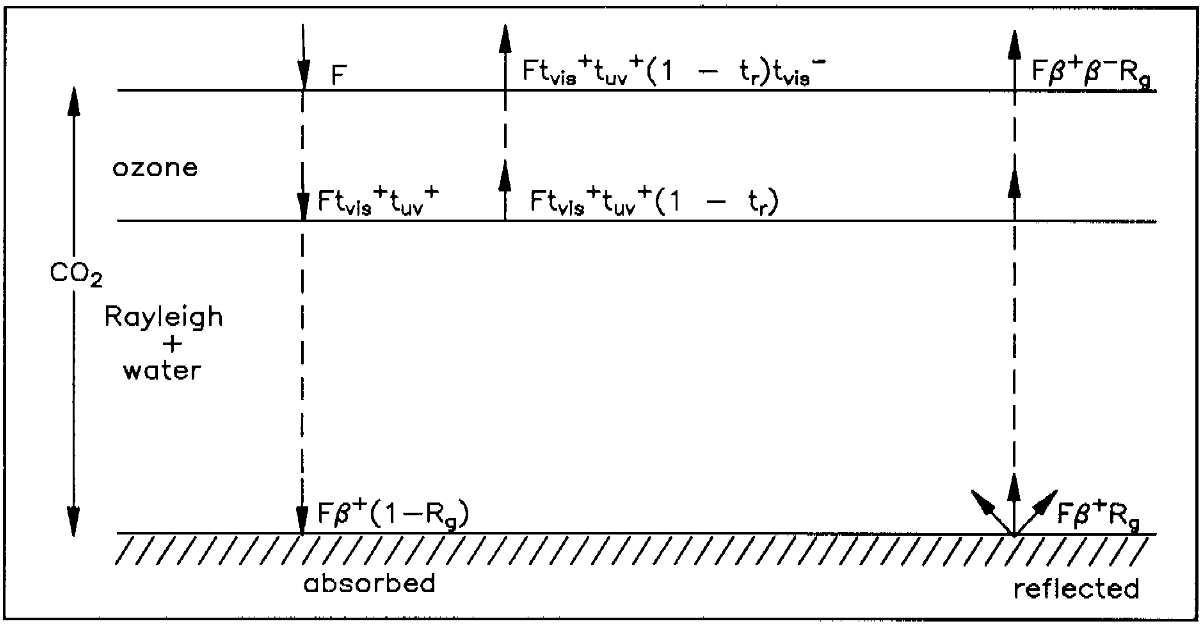

Figure 10. Clear sky solar flux transmission

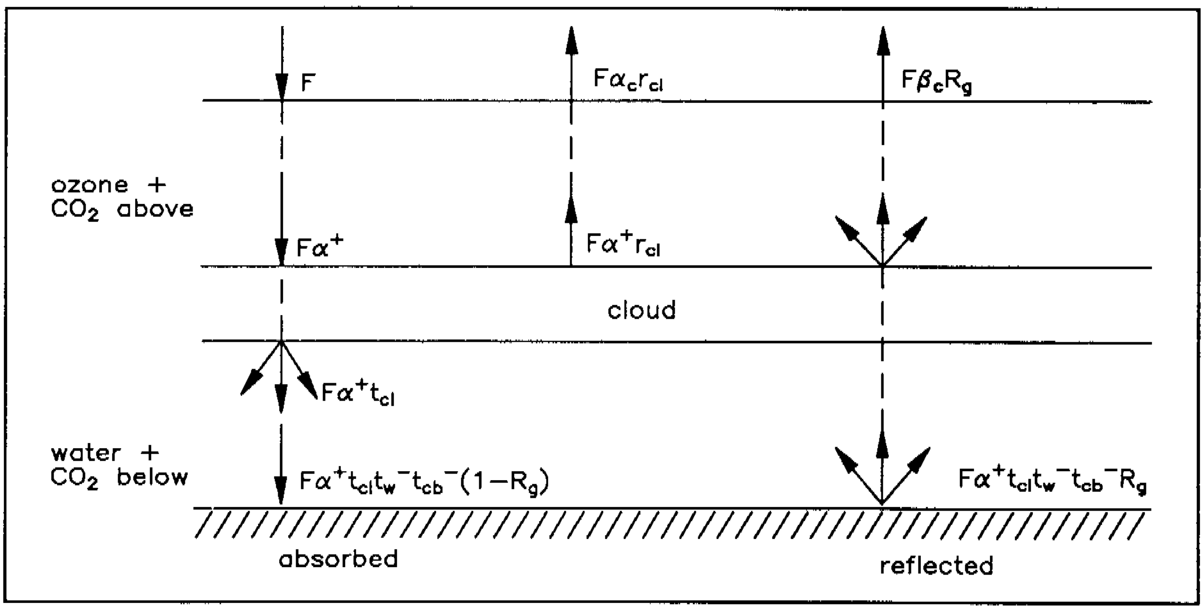

Figure 11. Cloudy sky solar flux transmission

incoming solar radiation. According to the CV model of Vardavas & Carver (1984*b*), t_{uv} can be approximated by:

$$t_{uv} = 1 - 0.023(W^*_{O3}/\bar{\mu})^{0.18} \tag{74}$$

and

$$t_{vis} = 1 - 0.021 W^*_{O3}/\bar{\mu} \tag{75}$$

where W^*_{O3} is now measured in cm-STP.

For incoming downward radiation, $\bar{\mu} = 1/2$, as was previously calculated. However solar radiation travelling in the upward direction has been diffused by contact with either the ground or clouds and so $\bar{\mu}$ is set to 3/5 which is the standard diffusivity approximation for converting diffuse transmission to equivalent direct transmission (e.g. see Kontratyev 1969). Both t_{vis} or t_{uv} agree well with fractions given in Lacis & Hansen (1974).

The second layer is a cloud layer with fractional cloud cover A_c (see Fig. 11). Each cloud type transmits a fraction t_{cl}. The simple two-stream approximation (Sagan & Pollack 1967) with no absorption is used so that t_{cl} is given by (see Lacis & Hansen 1974):

$$t_{cl} = 1 - R_{cl} \tag{76}$$

where R_{cl} is the cloud albedo given by:

$$R_{cl} = \frac{\sqrt{3}(1 - g_{cl})\tau_{cl}}{2 + \sqrt{3}(1 - g_{cl})\tau_{cl}} \tag{77}$$

where τ_{cl} is the cloud optical depth to solar radiation and g_{cl} is the asymmetry factor taken to be 0.85 in the present work.

The third layer is a Rayleigh scattering layer with water vapour absorption in the near infrared. Rayleigh scattering by air is important in the uv and visible but negligible in the near-infrared. The fraction t_R is transmitted after scattering and this fraction is set to a fixed value of 0.93 (e.g. Lacis & Hansen 1974) for both upward and downward radiation. Following Lacis & Hansen, Rayleigh scattering is ignored for the atmosphere beneath a cloud layer. Approximately 40% of incoming solar radiation is in the near-infrared (> 0.85 μm) so the minimum value of t_w is 0.60 (see Vardavas & Carver 1984*b*, table 6). From the complex model of Vardavas & Carver (1984),

$$t_w = 1 - 0.11\,(W^*_{H2O}/\bar{\mu})^{0.31} \tag{78}$$

using the Curtis-Godson approximation. The above expression is in close agreement with that of Yamamoto (1962).

The absorption of solar radiation by carbon dioxide takes place throughout the atmosphere. For a clear sky atmosphere the CV model gives:

$$t_c = 1 - 0.015\,(W^*_{CO2}/\bar{\mu})^{0.263} \tag{79}$$

For the total atmosphere the transmissivity, t_c, is computed with an absorber amount, W^*_{CO2}. Above a cloud layer the transmission, denoted by t_{ca}, is computed for an absorber amount $W^*_{CO2}\,(p_c/p_g)$ while below a cloud layer the transmission, denoted by t_{cb}, is computed for an absorber amount $W^*_{CO2}\,(1 - p_c/p_g)$.

The last layer is, in fact, an isotropically reflecting surface with a global mean albedo, R_g, of about 0.1 (e.g. Henderson-Sellers & Wilson 1983).

The planetary albedo R_p may be computed from:

$$R_p = 1 - a \tag{80}$$

where a is the absorption by the surface-atmosphere system:

$$a = (1 - A_c)a_s + \sum_i A_{ci}a_{ci} \tag{81}$$

where a_s is the planetary absorptivity for a clear sky and a_{ci} that for a cloud type i covering a fraction A_{ci} of the sky (assuming non-overlapping cloud cover components).

The derivation of the clear sky absorptivity, a_s, is shown in Fig. 10, where F represents the incoming solar radiation at the top of the atmosphere, $F_{IN}^{\downarrow}$.

The three solar flux components at the top of the atmosphere are: incoming, Rayleigh scattered and flux reflected by the earth.

For a clear sky:

$$a_s = 1 - t_{vis}^{+}\, t_{uv}^{+}(1 - t_R)t_{vis}^{-} - R_g\, \beta^{+}\beta^{-} \tag{82}$$

$$\text{where } \beta^{+} = t_R\, t_w^{+}\, t_c^{+}\, t_{vis}^{+}\, t_{uv}^{+} \ \text{ and } \ \beta^{-} = t_R\, t_w^{-}\, t_c^{-}\, t_{vis}^{-} \tag{83}$$

and the superscripts +/- refer to direct ($\bar{\mu}$ = 1/2) and diffuse ($\bar{\mu}$ = 3/5) radiation, respectively. The atmospheric transmission for upward uv flux, t_{uv}^{-}, is set to 1 since this flux component is negligible.

The deriviation of a_c is shown in Fig. 11 where below the cloud layer $\bar{\mu}$ = 3/5. Rayleigh scattering below a cloud layer is ignored because of downward re-scattering by the cloud cover. Above a multilayer cloud cover there is no simple way for including Rayleigh scattering. The error in the total outward flux that results from omitting this term is ~ 2%.

The solar flux components at the top of the atmosphere are incoming, cloud reflected and earth reflected. The cloud reflected flux is reduced by the ozone layer and CO_2 above the cloud while the earth reflected flux is reduced by ozone, cloud, CO_2, water and ground absorption.

The cloudy sky absorptivity, a_c, can be thus written as:

$$a_c = 1 - \alpha_c R_{cl} - \beta_c\, R_g \tag{84}$$

where $\alpha_c = \alpha^{+}\,\alpha^{-}$ with $\alpha^{+} = t_{uv}^{+}\, t_{vis}^{+}\, t_{ca}^{+}$, $\alpha^{-} = t_{vis}^{-}\, t_{ca}^{-}$
and $\beta_c = \alpha_c\, t_{cl}^{2}\, (t_w^{-}\, t_{cb}^{-})^2$

4.3 Flux at surface

In evaporation models, the net daily downward solar flux $\bar{F}_o^{\downarrow}(0)$ at the water surface is required and this can be computed, to a good approximation from:

$$\bar{F}_o^{\downarrow}(0) = F_{IN}^{\downarrow}\left[\,(1 - A_c)t_s^{*} + \sum_i A_{ci}\, t_{ci}^{*}\,\right] \tag{85}$$

where $t_s^{*} = (1 - R_g)\,\beta^{+}$ and $t_{ci}^{*} = (1 - R_g)\,\alpha^{+}\, t_{cl}\, t_w^{-}\, t_{cb}^{-}$

are the effective atmospheric transmissivity for a clear sky and through a cloudy sky for cloud type i, respectively (see Figs 10 & 11). For a waterbody $R_g \simeq 0.07$ is a reasonable estimate (e.g. Henderson-Sellers & Wilson 1983).

In terms of the fraction $fr_i = A_{ci}/A_c$ equation (85) can be re-written as:

$$\bar{F}_o^{\downarrow}(0) = \sum_i fr_i\, \bar{F}_o^{\downarrow}(0)_i \tag{86}$$

where $\bar{F}_o^{\downarrow}(0)_i = F_{IN}^{\downarrow}[(1-A_c)t_s^{*} + A_c t_{ci}^{*}]$

5 MODEL COMPUTATIONS

5.1 Method of solution

The model can be used to determine either the mean global surface temperature of the earth and the associated atmospheric radiation fluxes at the top and bottom of the atmosphere or these fluxes alone given local meteorological conditions and a specified surface temperature.

The atmosphere is divided into fixed pressure levels which define the atmospheric layers and altitudes of the cloud layers. This allows the τ grid structure of the atmosphere to be computed which then allows the following fluxes to be evaluated: $\overline{F}_o^{\downarrow}(\infty)$, the net downward solar flux at the top of the atmosphere; $\overline{F}_{ir}^{\uparrow}(\infty)$, the net upward terrestrial flux at the top of the atmosphere; $\overline{F}_o^{\downarrow}(0)$, the net downward solar flux at the surface; and $\overline{F}_{ir}^{\uparrow}(0)$, the net upward terrestrial flux at the surface.

Equation (1) can be solved iteratively for the surface temperature T_g by noting that $\overline{F}_{ir}^{\uparrow}(\infty) = \overline{t}_f\, \sigma T_g^4$ (equation 47) where $\overline{t}_f$ is dependent on T_g. The net incoming solar flux, $\overline{F}_o^{\downarrow}(\infty) = a\ F_{IN}^{\downarrow}$, can be taken as temperature independent so that the global mean surface temperature T_g can be obtained iteratively from:

$$T_g = [a\ F_{IN}^{\downarrow} \,/\, \overline{t}_f\, \sigma]^{\frac{1}{4}} \tag{87}$$

using Newton-Raphson iteration.

Note that the atmospheric optical depth due to water vapour, τ_{H2O}, depends on the total water vapour amount W_{H2O}^* and on the vertical water vapour profile which is determined by $\beta\ (T_g)$ (equation 20). If β is arbitrarily fixed to a particular value then equation (87) can be solved rapidly since $\overline{t}_f$ is then only weakly dependent on T_g. If β is solved consistently with T_g at each iteration then $\overline{t}_f$ is more strongly dependent on T_g.

5.2 Reference atmosphere

The output of this simple model (SV) is now compared with the more complex model (CV) of Vardavas & Carver (1984*b*). The CV model is a one-cloud single-layer model and so for comparison the SV model is run for a single cloud model.

The global mean surface temperature and the solar and terrestrial flux variations with cloud cover, carbon dioxide and water vapour that are predicted by the SV model are found to be in very good agreement with those of the CV model and with the work of other authors.

The CV reference atmospheric model was the present global mean atmosphere described by the following parameters:

$S_o = 1367\ Wm^{-2}\ (F_{IN}^{\downarrow} = 342\ Wm^{-2})$	$R_g = 0.1$
$W_{CO2}^* = 0.54\ g\ cm^{-2}$ (345 ppmm)	$W_{H2O}^* = 1.7\ g\ cm^{-2}$ (or precipitable cm)
$W_{O3}^* = 0.75 \times 10^{-3}\ g\ cm^{-2}$ (0.35 cm-STP)	$W_{CH4}^* = 0.9 \times 10^{-3}\ g\ cm^{-2}$ (1.6 ppmm)
$\Gamma = 6.5\ K\ km^{-1}$	$p_T = 200$ mbar
$A_c = 0.5$	$p_c = 530$ mbar
$\Delta p_c = p_{cb} - p_c = 20$ mbar	$\tau_c = 7.7$
$\varepsilon_g = 1$	$\varepsilon_c = 1$

For the above parameters it can be seen from Table 1 that the SV and CV model results are in very good agreement. The net incoming solar flux at the top of the atmosphere $\overline{F}_o^{\downarrow}(\infty) = 234.6$ W m^{-2} according to the SV reference model with $A_c = 0.5$ and 234.1 W m^{-2} according to the CV model. This is in agreement with the value of 234 ± 7 W m^{-2} given in Stephens et al. (1981) which is based on four years of satellite observations. The asymmetry factor g_{cl} was 0.85 for both the CV and SV model and the water vapour profile generated by the CV model was found to be best matched by the SV model using $\beta = 4$ in equation (15). For a clear sky atmosphere it can be seen from Table 1 that the two models are in close agreement.

The net downward solar flux at the surface $\overline{F}_o^{\downarrow}(0)$ is 172.0 W m^{-2} according to the SV reference model compared with 168.2 W m^{-2} given by the CV model, 160.0 W m^{-2} given by Peng et al. (1982) and 164.9 W m^{-2} given by Manabe & Strickler (1964). The downward atmospheric infrared flux $F_{ir}^{\downarrow}(0)$ at the surface is 320.7 W m^{-2} according to the SV model compared with 317.5 W m^{-2} for the CV model and 330.7 W m^{-2} given by Peng et al. (1982). Note that this flux depends crucially on the value assigned to W_{H2O}^*.

Table 1. Comparison of SV and CV model fluxes (W m^{-2}) and surface temperature (K)

	$A_c = 0$		$A_c = 0.5$		$A_c = 1$	
	SV	CV	SV	CV	SV	CV
$\overline{F}_o^{\downarrow}(\infty)$	299.5	296.8	234.6	234.1	169.6	171.3
$\overline{F}_o^{\downarrow}(0)$	227.9	223.1	172.0	168.2	116.1	113.5
$F_{ir}^{\downarrow}(0)$	327.3	327.4	320.7	317.5	289.7	285.1
T_g	296.1	296.9	287.8	288.2	275.0	275.2

5.3 Carbon dioxide effects

The variation of the global mean suface temperature T_g with atmospheric carbon dioxide (in PAL = present atmospheric level = 345 ppmm) is given in Fig. 12 with all other parameters fixed to those of the reference model. As can be seen there is a very good agreement between the CV model which predicts a temperature change $\Delta T_g = 1.3$ K and the SV model which predicts $\Delta T_g = 1.1$ K for a doubling of atmospheric carbon dioxide. The above changes in T_g are comparable to the lower range of values given in Climatic Change (1983) for global warming due to a doubling of the carbon dioxide and are in excellent agreement with the 1.2-1.3 K change given in Hansen et al. (1985) for a model with no climatic feedbacks. The variation of ΔT_g with carbon dioxide will be strongly influenced by the atmospheric water vapour and cloud cover feedbacks. As was discussed in Vardavas & Carver (1985), and shown in Fig. 12, the sensitivity of ΔT_g to a variation in carbon dioxide decreases with increasing atmospheric carbon dioxide due to the saturation of the strong carbon dioxide 15 μm bands. The increased sensitivity for concentrations $\leq$ 1 PAL could be an important factor in triggering recurrent ice ages on earth.

The change in the downward atmospheric infrared flux at the surface $\Delta F_{ir}^{\downarrow}(0)$ as a function of carbon dioxide amount is shown in Fig. 13. The SV and CV model results are in good agreement, both predicting $\simeq$ 6 W m^{-2} increase in the downward atmospheric infrared flux at the surface with doubling of CO_2. However, the increase in T_g results in an increase in the upward infrared flux emitted by the surface so that the net upward infrared flux at the surface decreases by $\simeq$ 0.5 W m^{-2}. In addition, the doubling of carbon dioxide results in a reduction in the downward solar flux at the surface by $\simeq$ 0.5 W m^{-2} so that the net gain of energy at the surface is close to zero.

In Fig. 14 are shown the effective ground infrared emissivities $\overline{\varepsilon}_g$ and $\overline{\varepsilon}_c$, equations (38) and (54), corresponding to a clear sky ($A_c = 0$) and a totally cloud covered ($A_c = 1$) sky, respectively, as functions of the atmospheric carbon dioxide amount. Both $\overline{\varepsilon}_g$ and $\overline{\varepsilon}_c$ exhibit

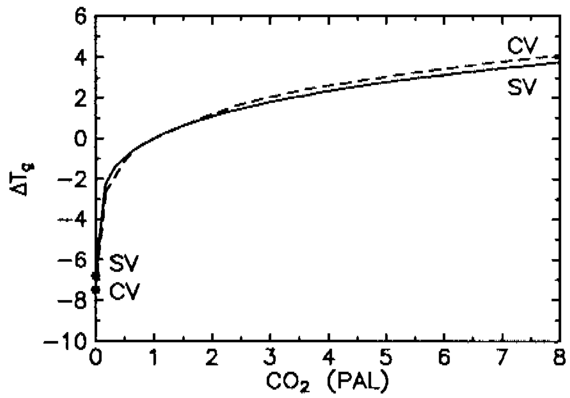

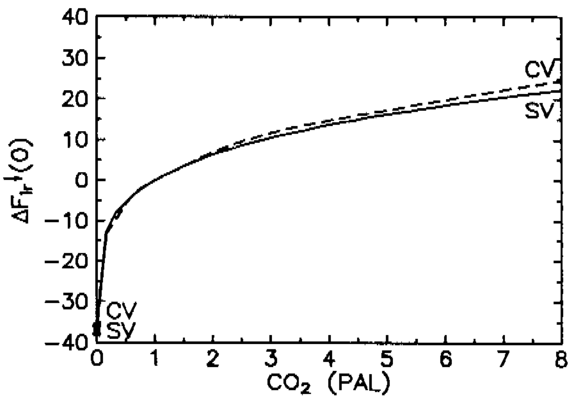

Figure 12. The global mean surface temperature change ΔT_g (K) as a function of atmospheric carbon dioxide amount in PAL (present atmospheric level = 345 ppmm) for the present simple (SV) and complex model (CV) of Vardavas & Carver (1984)

Figure 13. The change in global mean downward infrared flux (W m^{-2}) at the surface as a function of atmospheric carbon dioxide

a weak variation with carbon dioxide. Note that the values of $\bar{\varepsilon}_s$ and $\bar{\varepsilon}_c$ in Fig. 14 are for $\varepsilon_g = 1$, if these are denoted by $\bar{\varepsilon}_s(1)$ and $\bar{\varepsilon}_c(1)$, then in general:

$$\bar{\varepsilon}(\varepsilon_g) = \varepsilon_g\, \bar{\varepsilon}(1) \tag{88}$$

where

$$\bar{\varepsilon}(1) = (1-A_c)\, \bar{\varepsilon}_s(1) + A_c\, \bar{\varepsilon}_c(1)$$

For a water surface ε_g can lie between 0.9 and 1.0 (Beard & Hollen 1969; Hobson & Williams 1971) so that setting $\varepsilon_g = 1$ can result in a maximum error of about 10% in the net upward infrared flux.

In Fig. 14 are also shown the atmospheric transmissivities $\bar{t}_s$ and $\bar{t}_c$ (equations 36 & 45) for a clear sky and above a cloud layer, respectively. The SV and CV model results are once again in good agreement.

5.4 Water vapor effects

In Fig. 15 the effective emissivities $\bar{\varepsilon}_s$ (clear sky) and $\bar{\varepsilon}_c$ (under cloud cover) computed using $\varepsilon_g = 1$ are shown as functions of the atmospheric water vapour amount in g cm^{-2} or precipitable cm, keeping all other parameters fixed to their reference model values. The emissivities show a stronger variation with water vapour than they do with carbon dioxide. The SV and CV results are in good agreement for $W^*_{H2O} \geq 1$ cm, which is the region of interest for tropical and mid-latitudes. Atmospheric water vapour at any latitude is quite variable from one season to the next and when averaged annually it exhibits a decreasing trend with increasing latitude. In equatorial regions the mean annual value is 4.5 cm decreasing to $\simeq$ 1 cm at 60° latitude. In the wet/dry tropical northern Australia water vapour varies from $\simeq$ 2 cm during the Dry season to $\simeq$ 4 cm in the Wet.

The effective transmissivities $\bar{t}_s$ (clear sky) and $\bar{t}_c$ (above the cloud layer) also exhibit a stronger variation with water vapour than they do with carbon dioxide. Water vapour also affects appreciably the net incoming solar flux as can be seen from Fig. 16. The transmissivities t^*_s (clear sky) and t^*_c (total cloud cover) are shown and these describe net downward solar radiation at the surface, as defined by equation (85). The effective

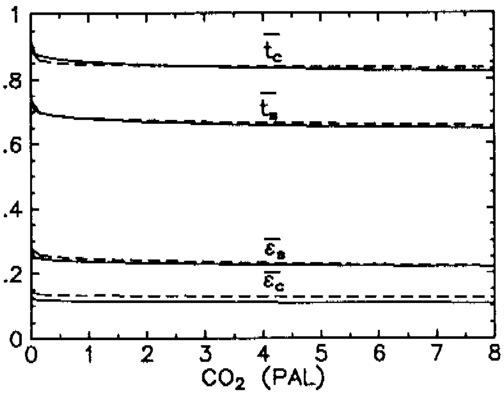

Figure 14. The effective surface infrared emissivities $\bar{\varepsilon}_s$ (under a clear sky) and $\bar{\varepsilon}_c$ (under a cloud layer) as functions of atmospheric carbon dioxide. The effective atmospheric infrared transmissivities $\bar{t}_s$ (clear sky) and $\bar{t}_{bc}$ (above cloud layer) are shown. SV____, CV_ _ _

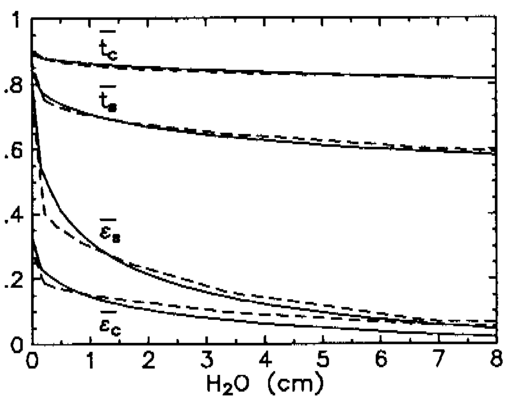

Figure 15. The effective surface infrared emissivities and atmospheric infrared transmissivities as functions of atmospheric water vapour in precipitable cm. SV____, CV_ _ _

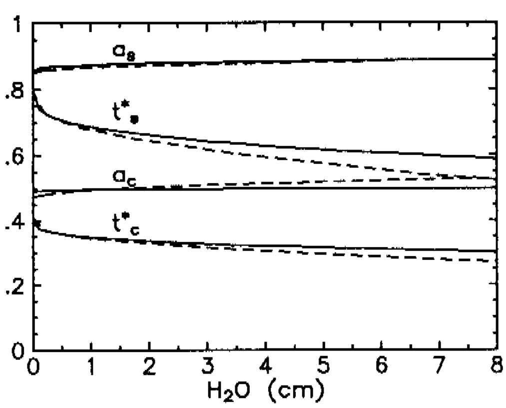

Figure 16. The effective planetary absorptivities a_s (clear sky) and a_c (total cloud cover) for solar radiation as functions of atmospheric water vapour (cm). The associated effective transmissivities t_s^* and t_c^* for solar radiation reaching the surface are also shown. SV____, CV_ _ _

absorptivities a_s (clear sky) and a_c (total cloud cover), which are functions of atmospheric water vapour (equations 82 and 84) and which determine the planetary albedo, are shown in Fig. 16.

The fraction f of the net downward solar flux at the surface which is lost by surface infrared emission is important to solar evaporation studies and can be written as:

$$f = \bar{F}_{ir}^{\uparrow}(0)/\bar{F}_{o}^{\downarrow}(0) \tag{89}$$

Recently, Huillet & Lauga (1985) have used a fixed value of 0.25 in their soil-plant-water model to compute solar evaporation in a forested catchment. From equation (89), f will depend on various meteorological quantities, amongst them cloud cover, incoming solar flux, surface temperature, carbon dioxide, water vapour and ground emissivity. The variation of f with water vapour is shown in Fig. 17 for the three surface temperatures 0, 15 and 30°C, for a clear sky atmosphere and with all other parameters set to those of the reference model. As the water vapour increases, the downward atmospheric flux increases and hence f decreases. The variation of f with Γ, A_c and carbon dioxide was found to be weak.

As $F_{IN}^{\downarrow}$ increases f will decrease so that, given a set of meterological conditions, f should be lower at the tropics than at mid-latitudes.

5.5 Latitudinal flux trends

The SV model was further tested by examining annually averaged latitudinal trends in the net downward solar flux and net upward infrared flux at the surface. The latitudinal trends were based on a model with $R_g = 0.1$, $\Gamma = 6.5$, $\tau_c = 7.7$ with the W_{H2O} (cm), W_{O3} (cm-STP) and A_c trends taken from Sasamori et al. (1972) for the southern hemisphere, an adopted T_g trend based on various sources and a computed $F_{IN}^{\downarrow}$ (W m^{-2}), as shown in Table 2 at each latitude L (degrees). In Fig. 18 the latitudinal variation of the net downward solar flux at the surface is shown, and it can be seen that there is good agreement with the trends of other workers (London

1957; Sasamori et al. 1972; Stephens et al. 1981). In Fig. 19 the trend of the net upward infrared flux at the surface is shown for ε_g = 1.0. As can be seen the SV model results are in close agreement with the variation given by Stephens et al. (1981) for the northern hemisphere. It should be borne in mind that the SV model computations are meant to show rough latitudinal trends, especially at high latitudes.

In Fig. 20 the annually averaged latitudinal trend of f is shown for ε_g = 1.0 and it can be seen that f increases from ~ 0.25 at tropical regions to ~ 0.6 at high latitudes. For artificial water reservoirs Beard & Hollen (1969) give ε_g = 0.922 so that setting ε_g = 1 can result in an ≃ 8% error in f.

Table 2. Model latitudinal trends in water vapour (cm), ozone (cm-STP), cloud cover, surface temperature (K) and incoming solar flux (W m^{-2})

L	W_{H2O}	W_{O3}	A_c	T_g	$F_{IN}^{\downarrow}$
0	4.2	0.26	0.48	305	415
10	3.7	0.27	0.48	300	410
20	2.9	0.28	0.48	295	394
30	2.2	0.31	0.50	290	367
40	1.6	0.33	0.59	285	331
50	1.2	0.35	0.72	280	288
60	0.8	0.35	0.83	275	241

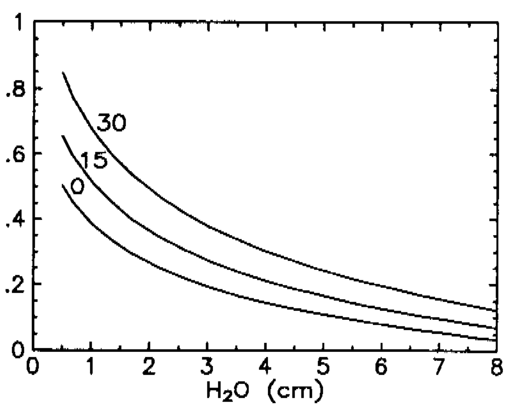

Figure 17. The fraction f of net solar radiation at the surface which is emitted as infrared radiation as a function of water vapour and surface temperatures 0, 15 and 30 (°C)

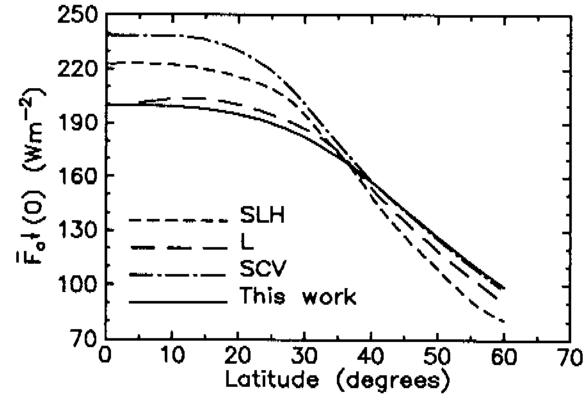

Figure 18. The latitudinal trend of net downward solar flux (W m^{-2}) at the surface given by the present SV model is compared with that of SCV (Stephens et al. 1981) and SLH (Sasamori et al. 1972) and L (London 1957)

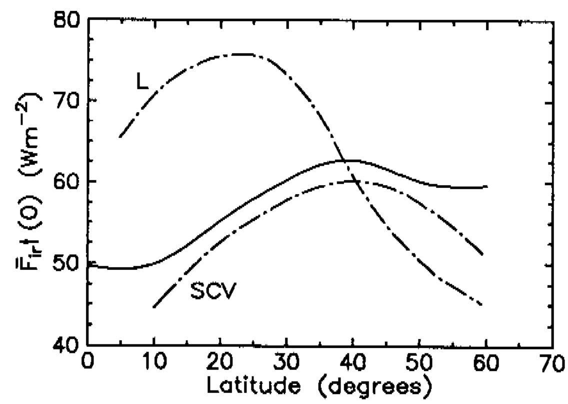

Figure 19. The latitudinal trend of net upward ir flux (W m^{-2}) at the surface, for ε_g = 1, given by the present SV model is compared with that given by L (London 1957) and SCV (Stephens et al. 1981)

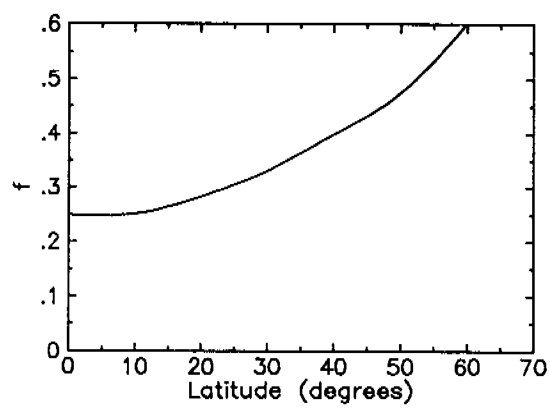

Figure 20. The latitudinal trend of the fraction f of net emitted infrared to net absorbed solar radiation by the surface for ε_g = 1

6 COMPUTER PROGRAMME

6.1 Programme modes and input data

The computer programme SRC (Simple Radiative-Convective) can be run in two modes: in the first mode it iteratively computes the mean global surface temperature and the solar and terrestrial fluxes at the top and bottom of the atmosphere, while in the second mode it computes the fluxes given site specific temperature conditions.

Mode A

The first mode requires mean global atmospheric conditions as input data and the iteration flag, ITF, is set to 1. The ground temperature is solved iteratively until flux balance at the top of the atmosphere is achieved. The initial estimate for the surface temperature is T_0.

Mode B

In the second mode, atmospheric data specific to a particular location are required, ITF is set to 0 which fixes the surface temperature at T_0. The fluxes at the top and bottom of the atmosphere are calculated for the given atmospheric data.

The input data are stored on a file called SRCIN and these are shown in the following table.

INPUT PARAMETERS

Text symbol	Computer name	Name	Units
$S_o = 1367$	So	Solar constant	$W\ m^{-2}$
μ	AMU	Mean cosine of solar zenith angle	
d	DAY	Day length	days
R_g	RG	Mean ground albedo to solar radiation	
W^*_{O3}	WO3	Atmospheric ozone amount	cm-STP
W^*_{H2O}	WH2O	Atmospheric water vapour amount	$g\ cm^{-2}$
W^*_{CH4}	WCH4	Atmospheric methane amount	$g\ cm^{-2}$
W^*_{CO2}	WCO2	Atmospheric carbon dioxide amount	$g\ cm^{-2}$
ε_g	EG	Ground infrared emissivity	
ε_{ci}	ECN(N) N=1,2,3	Cloud infrared emissivity	
pc_i	PCN(N)	Cloud top pressure	atmospheres
dpc_i	DPCN(N) N=1,2,3	Cloud thickness	mbar
τ_{ci}	CLTN(N) N=1,2,3	Cloud optical depth to solar radiation	
α_{ci}	CLAN(N)=0 N=1,2,3	Cloud absorption of solar radiation	
p_t	PT	Pressure at tropopause	mbar
T_o	TO	First estimate of surface temperature	K
Γ	GLAPZ	Lapse rate in troposphere	$K\ km^{-1}$
p_g	PG	Pressure at ground	mbar

Text symbol	Computer name	Name	Units
A_c	CC	Fractional cloud cover	
f_{ri}	FRN(N) N=1,2,3	Fraction of total cloud cover due to cloud type i	A_{ci}/A_c
r_{Hg}	RHO	Relative humidity at ground	
	ITF	Iteration flag	

6.2 Flow diagram

A flow diagram of the computer programme is given in Fig. 21. The programme first reads the input data file SRCIN then sets up the atmospheric pressure grid which defines the atmospheric layers and the location of the cloud layers, as shown in Fig. 22. The corresponding altitude grid, for a given atmospheric temperature structure, is then computed by a call to ZET. The programme then computes the terrestrial and solar fluxes for each cloud type by calls to subroutines TERRE and SOLAR, respectively. To compute the terrestrial fluxes, the programme needs to call three subroutines. Subroutine TAUS sets up the atmospheric optical depth grid, corresponding to the pressure grid. Subroutines HTAU and HINT then compute the integrals associated with the terrestrial flux transfer. Once the fluxes at the top and base of the atmosphere are known, the iteration flag ITF determines whether a global mean surface temperature will be computed iteratively via the Newton-Raphson temperature correction method. If ITF = 0 the programme run is for local atmospheric conditions and the programme exits via a call to ALTI which generates a table of the vertical atmospheric temperature and optical depth structure. If ITF = 1 the programme is automatically run once again with entry point the subroutine ZET which computes the altitude grid for a given atmospheric temperature structure. When the surface temperature, and hence temperature structure, converges (usually within about 5 iterations) the programme exits via a call to ALTI. The output is written on the file SRCOUT.

A detailed description of each programme subroutine now follows.

6.3 Main programme

The main programme first reads the input data and calculates $F_{IN}^{\downarrow}$. The parameters for the Newton-Raphson calculation of T_g are defined and shown in the following table. The main programme calls PGRID to set up the pressure grid. The temperature and altitude profiles are set up for the present value of T_g by calling subroutine ZET. The solar and terrestrial flux under each cloud type, both at the top and at the base of the atmosphere, are computed by calls to subroutines TERRE and SOLAR. The computed fluxes are: $\overline{F}_{ir}^{\uparrow}(0)_i$, $\overline{F}_{ir}^{\uparrow}(\infty)_i$, $\overline{F}_0^{\downarrow}(0)_i$, $\overline{F}_0^{\downarrow}(\infty)_i$ and are denoted in the programme by FIRG, FLOUT, FSOLG and FLIN, respectively. These fluxes are then summed over the 3 cloud types to give $\overline{F}_{ir}^{\uparrow}(0)$, $\overline{F}_{ir}^{\uparrow}(\infty)$, $\overline{F}_0^{\downarrow}(0)$ and $\overline{F}_0^{\downarrow}(\infty)$, denoted in the programme by sum5, sum2, sum4 and sum1, respectively.

At this point the programme can take three possible paths:

i) If ITF = 1 and if ER (see following table) is less than ε, then the net incoming solar flux effectively equals the outgoing terrestrial flux at the top of the atmosphere (i.e. radiative equilibrium). In this case the iterations stop and T_g is the global mean surface temperature.

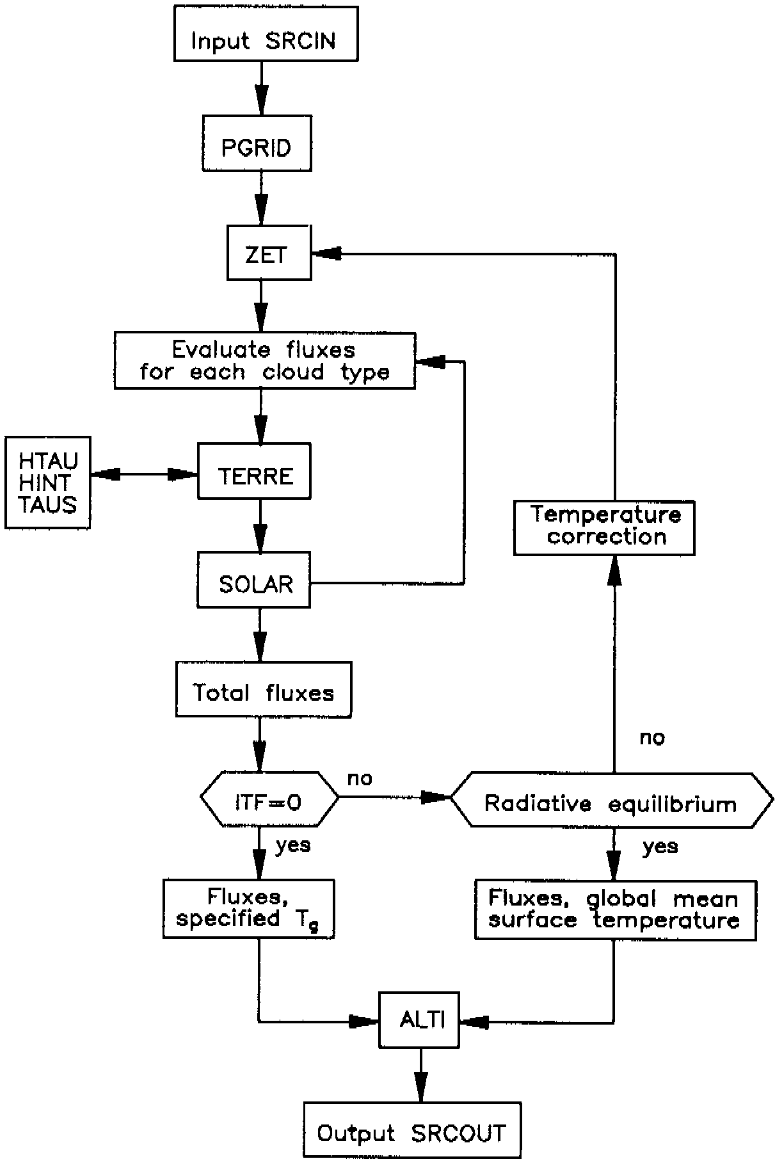

Figure 21. Flow diagram of the computer programme

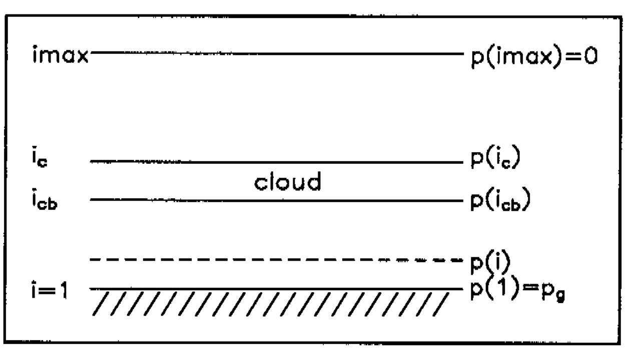

Figure 22. The pressure grid set up by subroutine PGRID

ii) If ITF = 1 and ER is greater than ε, then T_g needs to be corrected by ΔT until ER is less than ε. The temperature correction, ΔT, is calculated using the Newton-Raphson method:

$$\Delta T = \frac{G(T)}{G'(T)}, \quad \text{where } G(T) = \left| \overline{F}_o^{\downarrow}(\infty) - \overline{F}_{ir}^{\uparrow}(\infty) \right|$$

However G(T) is a complicated function of temperature T. So G'(T) is approximated by:

$$G'(T_k) = \frac{G(T_k) - G(T_{k-1})}{T_k - T_{k-1}}$$

where T_k is the ground temperature of the present iteration and T_{k-1} is that of the previous iteration. This gives at the kth iteration a temperature correction:

$$\Delta T_k = \frac{G(T_k)\ (T_k - T_{k-1})}{G(T_k) - G(T_{k-1})}$$

The temperature used in the next iteration is given by $T_{k+1} = T_k + \Delta T_k$. For k = 1 there is no value for T_{k-1} and ΔT_1 is arbitrarily set to 10.

The programme keeps iterating until ER < ε. In the programme $G(T_k)$, $G(T_{k-1})$, T_k, and T_{k-1} are denoted by GA, GB, TG and TGB, respectively.

iii) If ITF = 0 then the surface temperature is fixed at T_0. The solar and terrestrial fluxes at the top and bottom of the atmosphere are computed for this surface temperature.

MAIN PROGRAMME PARAMETERS

Text symbol	Computer name	Name	Units
$F_{IN}^{\downarrow}$	FLUX	Mean daily incoming solar flux at top of atmosphere	W m^{-2}
ε	EP	Maximum relative error allowed in flux balance equation	
	NMAX	Maximum number of iterations allowed	
	K	Iteration counter	
	ICB	Grid index for base of cloud	
	IC	Grid index for top of cloud	
$\overline{F}_o^{\downarrow}(\infty)_i$	FLIN	Net incoming solar flux at top of the atmosphere above cloud cover i	W m^{-2}
$\overline{F}_{ir}^{\uparrow}(\infty)_i$	FLOUT	Net outgoing terrestrial flux at top of the atmosphere above cloud cover i	W m^{-2}
$\overline{F}_o^{\downarrow}(0)_i$	FSOLG	Net downward solar flux at the ground below cloud cover i	W m^{-2}
$\overline{F}_{ir}^{\uparrow}(0)_i$	FIRG	Net upward terrestrial flux at the ground below cloud cover i	W m^{-2}
$\overline{F}_o^{\downarrow}(\infty)$	SUM1	Net incoming solar flux at top of the atmosphere	W m^{-2}
$\overline{F}_{ir}^{\uparrow}(\infty)$	SUM2	Net outgoing terrestrial flux at top of the atmosphere	W m^{-2}
$\overline{F}_o^{\downarrow}(0)$	SUM4	Net downward solar flux at ground	W m^{-2}
$\overline{F}_{ir}^{\uparrow}(0)$	SUM5	Net upward terrestrial flux at ground	W m^{-2}
$G(T_k)$	GA	$\lvert \overline{F}_o^{\downarrow}(\infty) - \overline{F}_{ir}^{\uparrow}(\infty) \rvert$ at iteration k.	W m^{-2}

Text symbol	Computer name	Name	Units
$G(T_{k-1})$	GB	$\lvert \overline{F}_o^{\downarrow}(\infty) - \overline{F}_{ir}^{\uparrow}(\infty) \rvert$ at iteration k-1.	$W\ m^{-2}$
T_k	TG	Ground temperature at iteration k	
T_{k-1}	TGB	Ground temperature at iteration k-1	
	ER	$ER = \lvert (\overline{F}_{ir}^{\uparrow}(\infty) - \overline{F}_o^{\downarrow}(\infty))/\overline{F}_o^{\downarrow}(\infty) \rvert$	
e_s	ES	Saturated water vapour pressure at ground	
β	BETA	Water vapour profile parameter (equation 20)	

6.4 Subroutines

Subroutine PGRID

Subroutine PGRID sets up a pressure grid and locates the cloud and tropopause levels. Between the ground ($p = p_g$) and the top of the atmosphere ($p = 0$) there are 100 layers of 10 mbar each. Each interval I, corresponds to a pressure p(I). At the ground I = 1, and at the top of the atmosphere I=IMAX=101. (See Fig. 22).

ICN(N) locates the top of cloud type N, where the cloud top pressure is P(ICN(N)) and N = 1,2,3 for three cloud types. Similarly, the interval at the base of cloud type N is called ICBN (N), with a pressure of p(ICBN(N)). The subroutine locates the tropopause with a pressure p(IT) $= p_T$.

Subroutine PGRID parameters

Computer name	Name	Units
DP	Pressure grid interval set equal to 10 mbar	mbar
ICN(N)	Level corresponding to the top of cloud type N	
PC=P(ICN(N))	Pressure at top of cloud type N	atmospheres
DPC	Cloud width	mbar
PCB=PC+DPC(N)	Pressure at bottom of cloud type N Note: PCB > PC	atmospheres
ICBN(N)	Level corresponding to base of cloud type N	

Subroutine ZET

ZET sets up the temperature versus pressure profile (equation 3) and the altitude versus pressure profile (equation 7). T_g, Γ, P_T and P_g are all given input parameters. The tropopause altitude corresponding to $p = p_T$ is calculated from equation (7).

Subroutine ZET parameters

Text symbol	Computer name	Name	Units
Γ	GLAPZ	Lapse rate = $-\,dT/dz$	$K\ km^{-1}$
g	GO=9.81	Gravitational acceleration	$m\ s^{-2}$
$\overline{M}$	AMW=28.97	Mean molecular weight of dry air	$g\ mol^{-1}$
R	R=8.314	Universal gas constant	$J\ mol^{-1}\ K^{-1}$
α	ALFA	$\alpha = \Gamma R/g\overline{M}$	-
$Z(p_t)$	ZT	Tropopause altitude	km

Subroutine ZET parameters (contd)

Text symbol	Computer name	Name	Units
p_t	PT	Tropopause pressure	mbar
	PI	P(I) mbar	
	PR	P(I)/PG -	
	IT	Tropopause level	-
	TT	Tropopause temperature	K

Subroutine TERRE

TERRE computes the net terrestrial flux at the top and base of the atmosphere by first evaluating $\overline{t}_c$, $\overline{t}_s$, $\overline{\varepsilon}_s$ and $\overline{\varepsilon}_c$ using subroutines HINT and TAUS. TAUS evaluates τ_c, τ_g and τ_{cb} for t_c, t_g and t_{cb}, while HINT evaluates the integrals. $\overline{F}_s^{\uparrow}(\infty)$, $\overline{F}_c^{\uparrow}(\infty)$, $\overline{F}_s^{\uparrow}(0)$ and $\overline{F}_c^{\uparrow}(0)$ are then found using equations 35, 44, 37 and 53. Finally $\overline{F}_{ir}^{\uparrow}(\infty)_i$ and $\overline{F}_{ir}^{\uparrow}(0)_i$ are evaluated using equations 48 and 58.

Subroutine TERRE parameters

Text symbol	Computer name	Name	Units
σ	SIG=5.6696 x 10^{-8}	Stefan-Boltzman constant	W m^{-2} K^{-4}
	TC	Temperature of cloud top	K
	TCB	Temperature of cloud base	K
τ_g	TAUG	$\tau(p_g,0)$	
τ_c	TAUC	$\tau(p_c,0)$	
τ_{cb}	TAUCB	$\tau(p_g,p_{cb})$	
t_g	TRG	Total atmospheric infrared transmissivity	
t_c	TRC	Atmospheric transmissivity above cloud layer	
t_{cb}	TRCB	Atmospheric transmissivity below cloud layer	
	FSOUT	Value of the first integral in $\overline{t}_s$	
	FSO	Value of the second integral in $\overline{t}_s$ or the integrals in $\overline{\varepsilon}_s$	
	FCOUT & FCUB	Value of the first and second integrals, respectively, in $\overline{t}_c$	
	FCDB & FCDA	Value of the integrals in the f_1 and f_2 terms of $\overline{\varepsilon}_c$	
$\overline{t}_s$	TBS	Effective atmospheric transmissivity for a clear sky (equation 36)	
$\overline{F}_s^{\uparrow}(\infty)$	FCL	$\overline{t}_s\varepsilon_g\sigma T_g^4$	W m^{-2}
$\overline{t}_{ci}$	TBC	Effective atmospheric transmissivity for a cloudy sky (equation 45)	
$\overline{F}_c^{\uparrow}(\infty)_i$	FAC	$\overline{t}_{ci}\varepsilon_{ci}\sigma T_c^4$	W m^{-2}
$\overline{F}_{ir}^{\uparrow}(\infty)_i$	FLOUT	Net outgoing terrestrial flux at the top of atmosphere for cloud type i (equation 47)	W m^{-2}
$\overline{\varepsilon}_c$	EBC	Effective ground emissivity below a cloud layer	W m^{-2}
$\overline{\varepsilon}_s$	EBS	Effective ground emissivity for a clear sky	
$\overline{F}_s^{\uparrow}(0)$	FBS	Net upward terrestrial flux at surface below a clear sky	W m^{-2}

Subroutine TERRE parameters (contd)

Text symbol	Computer name	Name	Units
$\overline{F}_{ir}^{\uparrow}(0)_i$	FIRG	Net upward terrestrial flux at surface below cloud i (equation 58)	W m^{-2}
	FBSD	Clear sky downward ir flux absorbed by ground	
	FBSU	Upward ir flux from the ground for a clear sky atmosphere. It is the sum of flux emitted by the ground plus terrestrial flux reflected by the ground	
	FBCD	Downward ir flux absorbed by ground below a cloudy sky atmosphere	
	FBCU	Upward ir flux from the ground for a cloudy sky. It is the sum of flux emitted from the ground plus terrestrial flux reflected by the ground	

Subroutine TAUS

TAUS determines the atmospheric optical depth, TAU, between pressure levels p(I1) and p(I2).

First the atmospheric water, carbon dioxide, methane and ozone amounts are found between the two specified pressure levels p(I1) and p(I2). For the evaluation of W^*_{O3} subroutine OZ is called. Finally the optical depths for the four types of molecules and the TAU are calculated using equations 32 and 33.

Subroutine TAUS parameters

Text symbol	Computer name	Name	Units
$c(T_g)$	FT	Optical depth temperature correction factor	
$G(z_1)$	OZF1	Green's function at z_1 (equation 26)	
$G(z_2)$	OZF2	Green's function at z_2	
W^*_{H2O}	WH2O	Total atmospheric water amount	g cm^{-2}
W^*_{CO2}	WC02	Total atmospheric carbon dioxide amount	g cm^{-2}
W^*_{O3}	WO3	Total atmospheric ozone amount	cm-STP
W^*_{CH4}	WCH4	Total atmospheric methane amount	g cm^{-2}
$W_{H2O}(p_1,p_2)$	WH	Water amount between p_1 and p_2 (equations 15)	g cm^{-2}
$W_{CO2}(p_1,p_2)$	WC	CO_2 amount between p_1 and p_2 (equation 23)	g cm^{-2}
$W_{CH4}(p_1,p_2)$	WCH	Methane amount between p_1 and p_2 (equation 24)	g cm^{-2}
$W_{O3}(p_1,p_2)$	WO	Ozone amount between p_1 and p_2 (equation 28)	cm-STP
$\tau_{H2O}(p_1,p_2)$	TAH	Optical depth of water between p_1 and p_2	
$\tau_{CO2}(p_1,p_2)$	TAC	CO_2 optical depth between p_1 and p_2	
$\tau_{O3}(p_1,p_2)$	TAO	O_3 optical depth between p_1 and p_2	
$\tau_{CH4}(p_1,p_2)$	TACH	CH_4 optical depth between p_1 and p_2	
$\tau(p_1,p_2)$	TAU	The total optical depth between p_1 and p_2	

Subroutine OZ

OZ computes Green's function G(Z) from equation (26). OZF is the computer name for G(z).

Subroutine HTAU

HTAU gives the integrand, $H(\tau)$, in the equations for $\overline{t}_s$, $\overline{t}_c$, $\overline{\varepsilon}_s$ and $\overline{\varepsilon}_c$ which takes the form:

$$H(\tau) = \left(\frac{T}{T_g}\right)^4 \exp(-\tau)$$

τ is specified by the subroutine HINT as τ(P(IP),P).

Subroutine HTAU parameters

Text symbol	Computer name	Name	Units
$H(\tau)$	HP	Integrand in flux equations	
τ	TAU	τ(P,P(IP))	
$T(\tau)$	T	Temperature at P	

Subroutine HINT

HINT evaluates the integrals, FIP, in the $\overline{t}_s$, $\overline{t}_c$, $\overline{\varepsilon}_s$ and $\overline{\varepsilon}_c$ equations. The integrals are evaluated using the trapezoidal rule. FIP represents the integral of $H(\tau)$ between layers defined by P(I1) and P(IM) evaluated for τ(P(IP), P(I)) where I ranges from IM to I1.

For example the second term of the $\overline{t}_s$ equation contains the integral:

$$= \int_0^{\tau_g} \left(\frac{T}{T_g}\right)^4 \exp(-\tau(0,p))d\tau$$

$$= \int_0^{\tau_g} H(\tau)d\tau, \qquad \tau = \tau(0,p)$$

Therefore,

τ(P(IP),P) = τ(0,p)

τ(P(IP),P(I1)) = $\tau(0,p_g) = \tau_g$

τ(P(IP),P(IM)) = 0

which gives IP = IMAX, I1 = 1 and IM = IMAX. This integral is evaluated in the programme by calling HINT (IMAX, 1, IMAX, FSOUT).

Subroutine SOLAR

SOLAR computes the net solar flux at the top and base of the atmosphere by first calculating atmospheric transmissivities. The cloud transmissivity is calculated with equation 76 and 77. The transmissivities of each absorber are solved using equations 74, 75, 78 and 79, for a given value of AMU = $\overline{\mu}^+$ for direct radiation. For diffuse radiation $\overline{\mu}^-$ is set equal to 3/5 whose inverse is 1.66. 'P' and 'M' as the last letter in the computer names refers to $\overline{\mu}$ equal to $\overline{\mu}^+$ and $\overline{\mu}^-$, respectively. The net solar flux at top and base of the atmosphere are determined from equation 73, 86. The computer names for the terms used are:

Subroutine SOLAR parameters

Text Symbol	Computer Name	Name
R_{CL}	RC	Cloud reflectivity
t_{CL}	CTR	Cloud transmissivity
$\alpha_{CL} = 0$	CLA	Cloud absorptivity (set to zero in this model)
$\overline{\mu}^+$		Direct radiation mean direction
$\overline{\mu}^-$		Diffuse radiation mean direction
${t_w}^+$	TWP	Water vapour transmissivity for direct radiation
${t_w}^-$	TWM	Water vapour transmissivity for diffused radiation
t^+_{vis}	TVP	Visible transmissivity for direct radiation
t^-_{vis}	TVM	Visible transmissivity for diffused radiation
t_{uv}	TUV	Ultraviolet transmissivity for direct downward radiation
t_R	TR = 0.93	Rayleigh scattering transmissivity (for both upward and downward radiation)
${t_{ca}}^+$	TCPP	t_{CO2} above cloudy sky for direct radiation
${t_{ca}}^-$	TCPM	t_{CO2} above cloudy sky for diffused radiation
${t_c}^+$	TCP	t_{CO2} for direct radiation for whole sky
${t_c}^-$	TCM	t_{CO2} for diffused radiation for whole sky
${t_{cb}}^-$	TCPD	t_{CO2} for diffused radiation below a cloudy sky
α^+	AP	$t_{uv}t^+_{vis}t^+_{ca}$
α^-	AM	$t^-_{vis}t^-_{ca}$
β^+	BP	$t_R t^+_w t^+_c t^+_{vis} t_{uv}$
β^-	BM	$t_R t^-_w t^-_c t^-_{vis}$
α_c	AA	$\alpha^+\alpha^-$
β_s	BB	$\beta^+\beta^-$
$t^-_w t^-_{ca}$	BC	
β_c	BD	$\alpha_c {t_{cl}}^2 (t^-_w\ t^-_{cb})^2$
a_s	AS	planetary absorptivity for a clear sky
a_{ci}	AC	planetary absorptivity for cloud type i
$a_{ci}F^{\downarrow}_{IN}$	FSC	Net incoming solar flux at top of the atmosphere for a cloudy sky for cloud type i
$a_s F^{\downarrow}_{IN}$	FSNC	Net incoming solar flux at top of the atmosphere for a clear sky
$\overline{F}^{\downarrow}_o(\infty)_i$	FLIN	Net incoming solar flux at top of atmosphere for cloud type i
$\overline{F}^{\downarrow}_o(0)_i$	FSOLG	Net downward solar flux at ground below cloud type i

Subroutine ALTI

ALTI writes the altitude, pressure, temperature, $\tau(p, p_g)$, $\tau(p, p_{cb})$, $\tau(p, p_c)$ and $\tau(p,0)$ for $0 \leq z \leq 30$ km and z = 100 km (for $z \rightarrow \infty$). These are described as z, p, T, TAP, TAUCB, TAC and TAUD in the programme.

6.5 Computer code

PROGRAM SRC

```
   COMMON /MT1/FLUX,CC,RG,EG
   COMMON /MT2/TG,TT,GLAPZ,PT,PG
   COMMON /MT3/IC,ICB,PC,DPC,CLT,CLA,EC,TC
   DIMENSION FRN(3),PCN(3),DPCN(3),CLTN(3),CLAN(3),ECN(3)
   DIMENSION ICN(3),ICBN(3)
   COMMON /SPEC/WCO2,WH2O,WO3,WCH4,BETA
   DATA SIG/5.6696E-8/
   OPEN(2,FILE='SRCOUT',STATUS='UNKNOWN')
   OPEN(3,FILE='SRCIN',STATUS='UNKNOWN')
   READ(3,23) SO,AMU,DAY,RG,EG,PG
  C,GLAPZ,PT,CC
  C,WCO2,WH2O,WO3,WCH4,RHO
  C,(PCN(N),N=1,3)
  C,(DPCN(N),N=1,3)
  C,(CLTN(N),N=1,3)
  C,(CLAN(N),N=1,3)
  C,(ECN(N),N=1,3)
  C,(FRN(N),N=1,3)
  C,TO,ITF
23 FORMAT(33(8X,F9.4,/),8X,I2)
   FLUX=AMU*DAY*SO
   WRITE(2,19)
   WRITE(2,20)
19 FORMAT(1H1,50X,'SIMPLE CLIMATE MODEL',///)
20 FORMAT(4X,'SO',6X,'AMU',3X,'DAY',4X,'RG',3X,'FLUX',
  C5X,'CC',3X,'WH2O',3X,'WCO2',4X,'WO3',
  C3X,'WCH4',5X,'LAP',3X,'PT',7X,'EG',3X,'RHO',/)
   WRITE(2,10) SO,AMU,DAY,RG,FLUX,CC,WH2O,WCO2,WO3,
  CWCH4,GLAPZ,PT,EG,RHO
10 FORMAT(2X,F7.2,3(2X,F4.2),2X,F7.2,2X,F4.2,
  C3(2X,F5.2),2X,F7.5,2X,F4.1,2X,F4.0,2(3X,F4.2))
   WRITE(2,21)
   WRITE(2,22) (PCN(N),N=1,3),(DPCN(N),N=1,3),(CLTN(N),N=1,3),
  C(CLAN(N),N=1,3),(ECN(N),N=1,3),(FRN(N),N=1,3)
21 FORMAT(//,10X,'CLOUD PROPERTIES'//,9X,'LOW',5X,'MIDDLE',3X,'HIGH')
22 FORMAT(//,3X,'PC',3(4X,F4.2)/2X,'DPC',3(4X,F4.1)/2X,'CLT',
  C3(4X,F4.1)/2X,'CLA',3(4X,F4.1)/3X,'EC',3(4X,F4.2)/3X,'FR',
  C3(4X,F4.2)///)
   EP=0.0001
   NMAX=20
   TG=TO
   CALL PGRID(PCN,DPCN,ICN,ICBN)
   K=0
 1 CONTINUE
   K=K+1
   WRITE(2,*)
```

```
      WRITE(2,*) ' ITERATION = ',K
      ALES=58.1717-6938.67/TG-5.5189*ALOG(TG)
      ES=EXP(ALES)
      BETA=0.634*RHO*ES/WH2O-1
      WRITE(2,*) ' TG = ',TG,' BETA = ',BETA
      CALL ZET
      SUM1=0
      SUM2=0
      SUM3=0
      SUM4=0
      SUM5=0
      DO 4 N=1,3
      WRITE(2,*)
      IF(N.EQ.1) WRITE(2,*) ' LOW CLOUD'
      IF(N.EQ.2) WRITE(2,*) ' MIDDLE CLOUD'
      IF(N.EQ.3) WRITE(2,*) ' HIGH CLOUD'
      ICB=ICBN(N)
      IC=ICN(N)
      PC=PCN(N)*PG
      DPC=DPCN(N)
      CLT=CLTN(N)
      CLA=CLAN(N)
      EC=ECN(N)
      CALL SOLAR(AMU,FLIN,FSOLG,TSTARS,TSTARC,AS,AC)
      CALL TERRE(ITF,FLOUT,FIRG,TBS,TBC,EBS,EBC)
      SUM1=SUM1+FRN(N)*FLIN
      SUM2=SUM2+FRN(N)*FLOUT
      SUM4=SUM4+FRN(N)*FSOLG
      SUM5=SUM5+FRN(N)*FIRG
    4 CONTINUE
      GA=SUM2-SUM1
      DT=-GA*(TG-TGB)/(GA-GB)
      TGB=TG
      IF(K.EQ.1) TG=TGB+10
      IF(K.GT.1) TG=TGB+DT
      GB=GA
      IF(ITF.EQ.0) TG=T0
      ER=ABS((SUM2-SUM1)/SUM1)
      WRITE(2,*) K,SUM1,SUM2,DT,TG,ER
      WRITE(2,*) ' NET IR OUT = ',SUM2,' NET SOL IN = ',SUM1
      WRITE(2,*) ' NET SOLG DOWN = ',SUM4,' NET IRG UP = ',SUM5
      EGST4=EG*SIG*TG**4
      WRITE(2,*) ' GROUND EMISSION = ',EGST4
      IF(K.LT.NMAX.AND.ER.GT.EP.AND.ITF.EQ.1) GO TO 1
      IF(ER.GT.EP.AND.ITF.EQ.1) WRITE(2,*) ' NO CONVERGENCE '
    5 CONTINUE
      IF(ITF.EQ.1) WRITE(2,*) ' ITF=1: SURFACE TEMPERATURE COMPUTED'
      IF(ITF.EQ.0) WRITE(2,*) ' ITF=0: SURFACE TEMPERATURE SPECIFIED'
      CALL ALTI
      STOP
      END
```

SUBROUTINE TERRE(ITF,FLOUT,FIRG,TBS,TBC,EBS,EBC)

```
      COMMON /SPEC/WCO2,WH2O,WO3,WCH4,BETA
      COMMON /MT1/FLUX,CC,RG,EG
```

```
COMMON /MT2/TG,TT,GLAPZ,PT,PG
COMMON /MT3/IC,ICB,PC,DPC,CLT,CLA,EC,TC
COMMON /PTC/P(101),T(101),Z(101),IMAX,IT
DATA SIG/5.6696E-8/
TC=T(IC)
CALL TAUS(1,IMAX,TAUG)
CALL TAUS(IC,IMAX,TAUC)
CALL TAUS(1,ICB,TAUCB)
TRG=EXP(-TAUG)
TRC=EXP(-TAUC)
TRCB=EXP(-TAUCB)
T4=TG**4
TC4=TC**4
WRITE(2,*) TG,TC,TT,TAUG,TAUC
CALL HINT(IMAX,1,IMAX,FSOUT)
CALL HINT(IMAX,IC,IMAX,FCOUT)
CALL HINT(1,1,IMAX,FSO)
CALL HINT(ICB,1,ICB,FCUB)
CALL HINT(1,1,ICB,FCDB)
CALL HINT(IC,IC,IMAX,FCDA)
EGST4=EG*SIG*T4
TBS=TRG+FSOUT/EG-(1-EG)*TRG*FSO/EG
FCL=TBS*EGST4
TBC=TRC+(T4/TC4)*FCOUT/EC+(1-EC)*(FCUB+EG*TRCB)*TRC*T4/(EC*TC4)
FAC=TBC*EC*SIG*TC4
FLOUT=(1-CC)*FCL+CC*FAC
WRITE(2,*) TBS,TBC
WRITE(2,*) ' IROUT CLEAR = ',FCL,' IROUT CLOUD = ',FAC
WRITE(2,*) ' IROUT TOTAL = ',FLOUT
FBSD=EGST4*(-FSO)
FBSU=EGST4+(1-EG)*FBSD/EG
FBS=FBSU-FBSD
FBCD=EGST4*(-FCDB+EC*(TC4/T4)*TRCB-(1-EC)*FCDA*trcb)
FBCU=EGST4+(1-EG)*FBCD/EG
FBC=FBCU-FBCD
EBC=FBC/(SIG*T4)
EBS=FBS/(SIG*T4)
WRITE(2,*) EBS,EBC
FIRG=(1-CC)*FBS+CC*FBC
WRITE(2,*) FBS,FB,CC,FIRG
RETURN
END
```

SUBROUTINE SOLAR(AMU,FLIN,FSOLG,TSTARS,TSTARC,AS,AC)

```
COMMON /SPEC/WCO2,WH2O,WO3,WCH4,BETA
COMMON /MT1/FLUX,CC,RG,EG
COMMON /MT2/TG,TT,GLAPZ,PT,PG
COMMON /MT3/IC,ICB,PC,DPC,CLT,CLA,EC,TC
DATA SIG/5.6696E-8/,TR/0.93/
DATA GS/0.85/,R3/1.732/
PCG=PC/PG
R3G=R3*(1-GS)*CLT
RC=R3G/(2+R3G)
CTR=1-RC-CLA
TWP=1-.11*(WH2O/AMU)**0.31
```

```
      TWM=1-.11*(1.66*WH2O)**0.31
      TVP=1-.021*WO3/AMU
      TVM=1-.021*1.66*WO3
      TUV=1-0.023*(WO3/AMU)**0.18
      TCPP=1-0.015*(WCO2*PCG/AMU)**0.263
      TCPM=1-0.015*(WCO2*PCG*1.66)**0.263
      TCP=1-0.015*(WCO2/AMU)**0.263
      TCM=1-0.015*(1.66*WCO2)**0.263
      TCPD=1-0.015*(WCO2*(1-PCG)*1.66)**0.263
      AP=TUV*TVP*TCPP
      AM=TVM*TCPM
      BP=TR*TWP*TCP*TVP*TUV
      BM=TR*TWM*TCM*TVM
      AA=AP*AM
      BB=BP*BM
      BC=TWM*TCPD
      BD=AA*CTR*CTR*BC*BC
      AC=1-AA*RC-BD*RG
      FSC=FLUX*AC
      AS=1-(1-TR)*TUV*TVP*TVM-BB*RG
      FSNC=FLUX*AS
      FLIN=CC*FSC+(1-CC)*FSNC
      TSTARS=BP*(1-RG)
      TSTARC=AP*CTR*BC*(1-RG)
      FSOLG=(1-CC)*FLUX*TSTARS+CC*FLUX*TSTARC
      RETURN
      END
```

SUBROUTINE HINT(IP,I1,IM,FIP)

```
      DIMENSION TAUP(101)
      COMMON /PTC/P(101),T(101),Z(101),IMAX,IT
      DO 2 I=1,IMAX
      CALL TAUS(IP,I,TAU)
      TAUP(I)=TAU
    2 CONTINUE
      I2=I1+1
      IM1=IM-1
      DP=TAUP(I2)-TAUP(I1)
      TP=T(I1)
      TAUPP=TAUP(I1)
      CALL HTAU(TP,TAUPP,HP)
      SUM1=-DP*HP/2
      DO 1 I=I2,IM1
      DP=TAUP(I+1)-TAUP(I-1)
      TP=T(I)
      TAUPP=TAUP(I)
      CALL HTAU(TP,TAUPP,HP)
      SUM1=SUM1-DP*HP/2
    1 CONTINUE
      DP=TAUP(IM)-TAUP(IM1)
      TP=T(IM)
      TAUPP=TAUP(IM)
      CALL HTAU(TP,TAUPP,HP)
```

```
      FIP=SUM1-DP*HP/2
      WRITE(2,*) '  FIP =',FIP
      RETURN
      END
```

SUBROUTINE PGRID(PCN,DPCN,ICN,ICBN)

```
      DIMENSION PCN(3),DPCN(3),ICN(3),ICBN(3)
      COMMON /PTC/P(101),T(101),Z(101),IMAX,IT
      COMMON /MT2/TG,TT,GLAPZ,PT,PG
      IMAX=101
      DP=PG/(IMAX-1)
      P(1)=PG
      DO 1 I=1,IMAX
      P(I)=PG-DP*(I-1)
      DO 2 N=1,3
      PC=PCN(N)*PG
      PCB=PC+DPCN(N)
      IF(P(I).EQ.PC) ICN(N)=I
      IF(P(I).EQ.PCB) ICBN(N)=I
    2 CONTINUE
      IF(P(I).EQ.PT) IT=I
    1 CONTINUE
      RETURN
      END
```

SUBROUTINE TAUS(I1,I2,TAU)

```
      COMMON /SPEC/WCO2,WH2O,WO3,WCH4,BETA
      COMMON /PTC/P(101),T(101),Z(101),IMAX,IT
      P1=P(I1)
      P2=P(I2)
      PG=P(1)
      Z1=Z(I1)
      Z2=Z(I2)
      CALL OZ(Z1,OZF1)
      CALL OZ(Z2,OZF2)
      FT=-0.0045*T(1)+2.3
      PR=ABS((P1-P2)/PG)
      PR5=(P1/PG)**(1+BETA)-(P2/PG)**(1+BETA)
      PR5=ABS(PR5)
      WH=WH2O*PR5
      WC=WCO2*PR
      WO=0.00214*WO3*ABS(OZF1-OZF2)
      WCH=WCH4*PR
      TAH=0.63*WH**0.52
      TAC=0.14*WC**0.22
      TAO=2.51*WO**0.62
      TACH=2.51*WCH**0.75
      TAU=1.66*FT*(TAH+TAC+TAO+TACH)
      RETURN
      END
```

SUBROUTINE ZET

```
      COMMON /MT2/TG,TT,GLAPZ,PT,PG
      COMMON /PTC/P(101),T(101),Z(101),IMAX,IT
      DATA G0/9.80665/,AMW/28.97/,R/8.314/
      ALFA=GLAPZ*R/(G0*AMW)
      ZT=TG*(1-(PT/PG)**ALFA)/GLAPZ
      IMAX1=IMAX-1
      DO 1 I=1,IMAX1
      PI=P(I)
      PR=PI/PG
      IF(PI.GE.PT) Z(I)=TG*(1-PR**ALFA)/GLAPZ
      T(I)=TG-GLAPZ*Z(I)
      IF(PI.LT.PT) T(I)=TG-GLAPZ*ZT
      IF(PI.LT.PT) Z(I)=ZT-ALOG(PI/PT)*ALFA*T(I)/GLAPZ
      IF(Z(I).EQ.ZT) IT=I
    1 CONTINUE
      TT=T(IT)
      Z(IMAX)=100.
      T(IMAX)=TG-GLAPZ*ZT
      RETURN
      END
```

SUBROUTINE OZ(Z,OZF)

```
      DATA B/20./,C/5./
      AN=1+EXP(-B/C)
      DEN=1+EXP((Z-B)/C)
      OZF=AN/DEN
      RETURN
      END
```

SUBROUTINE HTAU(T,TAU,HP)

```
      COMMON /MT2/TG,TT,GLAPZ,PT,PG
      HP=EXP(-TAU)*((T/TG)**4)
      RETURN
      END
```

SUBROUTINE ALTI

```
      COMMON /PTC/P(101),T(101),Z(101),IMAX,IT
      COMMON /MT3/IC,ICB,PC,DPC,CLT,CLA,EC,TC
      WRITE(2,19)
   19 FORMAT(/////,20X,'VERTICAL STRUCTURE',//)
      WRITE(2,20)
   20 FORMAT(4X,'Z',7X,'P',5X,' T ',6X,'TAP',5X,'TACB',
     C4X,' TAC',3X,' TAUD')
      DO 1 I=1,IMAX
      CALL TAUS(1,I,TAP)
      CALL TAUS(I,ICB,TACB)
      CALL TAUS(I,IC,TAC)
      CALL TAUS(I,IMAX,TAUD)
      CALL HTAU(T(I),TAP,HP)
```

```
   CALL HTAU(T(I),TAUD,HM)
   FT=-0.0045*T(1)+2.3
30 FORMAT(5(2X,F6.4))
   WRITE(2,21) Z(I),P(I),T(I),TAP,TACB,TAC,TAUD
21 FORMAT(2X,F4.1,2(2X,F7.2),4(2X,F6.4))
 1 CONTINUE
   RETURN
   END
```

6.6 Samples of input/output

Sample input data files are given as: SRCINA (global mean) and SRCINB (specific location). For SRCINA, ITF = 1 and T_o = 270 K. As can be seen in the output file SRCOUTA the program converges to the mean global temperature (T_g = 288.46 K) in 5 iterations and the net inward solar flux at the top of the atmosphere equals 228 Wm^{-2}. For SCRINB, ITF = 0 and T_o is fixed at 288.5 K. The fluxes $\overline{F}_{ir}^{\uparrow}(\infty)$, $\overline{F}_{0}^{\downarrow}(\infty)$, $\overline{F}_{ir}^{\uparrow}(0)$ and $\overline{F}_{0}^{\downarrow}(0)$ are computed for both cases. The corresponding output files are SRCOUTA and SRCOUTB.

Input for a 3 cloud model, with ITF = 1
Global average conditions
Filename = SRCINA

So	=	1367.0	solar constant (Wm^{-2})
Mu	=	0.5	$\bar{\mu}$ = daily mean cosine of solar zenith angle
Day	=	0.5	daylength in days
Rg	=	0.13	ground albedo
Eg	=	1.00	ground infrared emissivity
Pg	=	1000.	ground atmospheric pressure
Gam	=	6.5	lapse rate = $\Gamma = -dT/dz$ (K km^{-1})
Pt	=	200.	pressure of tropopause (mbar)
Ac	=	0.54	fractional cloud cover
CO2	=	0.54	W^*_{CO2} = total atmospheric CO_2 amount (gm cm^{-2})
H2O	=	2.17	W^*_{H2O} = total atmospheric H_2O amount (gm cm^{-2})
O3	=	.31	W^*_{O3} = total atmospheric O_3 amount (cm-STP)
CH4	=	.0009	W^*_{CH4} = total atmospheric CH_4 amount (gm cm^{-2})
rh0	=	0.77	relative humidity at surface
Pcl	=	0.76	
Pcm	=	0.56	pressure height at cloud top (atmospheres)
Pch	=	0.20	
Dpcl	=	100.	
Dpcm	=	50.	cloud thickness in mbar
Dpch	=	70.	
Tcl	=	20.0	
Tcm	=	15.0	cloud optical depth to solar radiation
Tch	=	2.0	
Tal	=	0.	
Tam	=	0.	cloud absorption of solar radiation is ignored
Tah	=	0.	
Ecl	=	1.0	
Ecm	=	1.0	cloud emissivity in infrared
Ech	=	0.3	

Frl	=	0.34	cloud type fractional cover	
Frm	=	0.28		
Frh	=	0.38		
To	=	270.0	surface temperature first guess (K)	
ITF	=	1	iteration flag ITF = 1:	solves for surface temperature
			ITF = 0:	specified temperature

Output for a 3 cloud model, with ITF = 1
Global average conditions
Filename = SRCOUTA

SIMPLE CLIMATE MODEL

S0	AMU	DAY	RG	FLUX	CC	WH2O	WCO2	WO3	WCH4	LAP	PT	EG	RH0
1367.	.50	.50	.13	341.75	.54	2.17	.54	.31	.00090	6.5	200.	1.00	.77

CLOUD PROPERTIES

	LOW	MIDDLE	HIGH
PC	.76	.56	.20
DPC	100.	50.0	70.0
CLT	20.0	15.0	2.0
CLA	0.0	0.0	0.0
EC	1.00	1.00	.30
FR	.34	.28	.38

```
ITERATION = 1
TG = 270. BETA = 8.76284E-2

LOW CLOUD

   TG            TC          TT        TAUG       TAUC
  270.         256.27      198.8      1.9897     1.7281
FIP = .32794
FIP = .29111
FIP = -.7403
FIP = .50152
FIP = -.53044
FIP = -.56617
   TBS            TBC
.46468         .53633
IROUT CLEAR = 140.01 IROUT CLOUD =  131.15
IROUT TOTAL = 135.22
   EBS            EBC
 .2597          .09970
```

```
   FBS           FBC         CC      FIRG
78.249        30.041        .54    52.216

MIDDLE CLOUD
    TG            TC          TT      TAUG       TAUC
  270.          241.8       198.8    1.9897     1.4797
FIP = .32794
FIP = .25489
FIP = -.7403
FIP = .54682
FIP = -.6718
FIP = -.41922
TBS             TBC
.46468        .62395
IROUT CLEAR = 140.01 IROUT CLOUD = 120.94
IROUT TOTAL = 129.71
EBS             EBC
 .2597        .14764
   FBS           FBC         CC      FIRG
78.249        44.484        .54    60.016

HIGH CLOUD
    TG            TC          TT      TAUG       TAUC
  270.          198.8       198.8    1.9897     .88926
FIP = .32794
FIP = .17337
FIP = -.7403
FIP = .41462
FIP = -.7266
FIP = -.17341
TBS             TBC
.46468         4.323
IROUT CLEAR = 140.01 IROUT CLOUD = 114.84
IROUT TOTAL = 126.42
EBS             EBC
 .2597        .23534
   FBS           FBC         CC      FIRG
78.249        70.909        .54    74.286
K  SUM1         SUM2         DT        TG         ER
1  227.89     130.33       -270.      280.     .42808
NET IR OUT = 130.33 NET SOL IN = 227.89
NET SOLG DOWN = 162.21 NET IRG UP = 62.787
GROUND EMISSION = 348.49

ITERATION = 2
TG = 280. BETA = 1.228

LOW CLOUD
    TG            TC          TT      TAUG       TAUC
  280.         265.76      206.16    1.9072     1.4471
FIP = .3975
FIP = .31942
FIP = -.77368
FIP = .58
FIP = -.61506
FIP = -.55318
```

```
TBS              TBC
  .546         .62883
IROUT CLEAR = 190.27 IROUT CLOUD = 177.84
IROUT TOTAL = 183.56
EBS              EBC
.22632         .08386
   FBS             FBC          CC       FIRG
78.869         29.226          .54     52.062

MIDDLE CLOUD
    TG             TC           TT        TAUG        TAUC
  280.         250.76       206.16      1.9072      1.0772
FIP = .3975
FIP = .2432
FIP = -.77368
FIP = .59523
FIP = -.73623
FIP = -.37252
TBS              TBC
  .546         .71861
IROUT CLEAR = 190.27 IROUT CLOUD = 161.09
IROUT TOTAL = 174.52
EBS              EBC
.22632         .12104
   FBS             FBC          CC       FIRG
78.869         42.179          .54     59.057

HIGH CLOUD
    TG             TC           TT        TAUG        TAUC
  280.         206.16       206.16      1.9072      .44938
FIP = .3975
FIP = .1064
FIP = -.77368
FIP = .45855
FIP = -.76884
FIP = -.10647
TBS              TBC
  .546           5.
IROUT CLEAR = 190.27 IROUT CLOUD = 153.62
IROUT TOTAL = 170.48
EBS              EBC
.22632         .20443
   FBS             FBC          CC       FIRG
78.869          71.24          .54     74.749
K  SUM1          SUM2          DT         TG           ER
2  227.89      176.06       11.335     291.34      .22743
NET IR OUT = 176.06 NET SOL IN = 227.89
NET SOLG DOWN = 162.21 NET IRG UP = 62.641
GROUND EMISSION = 408.44

ITERATION = 3
TG = 291.34 BETA = 3.6938

LOW CLOUD
    TG             TC           TT        TAUG        TAUC
291.34         276.52        214.5      1.8136      1.0421
FIP = .49661
```

```
FIP = .32579
FIP = -.79221
FIP = .65187
FIP = -.69444
FIP = -.48122
TBS             TBC
.65968        .75414
IROUT CLEAR = 269.44 IROUT CLOUD = 249.97
IROUT TOTAL = 258.92
EBS             EBC
.20779        .06696
   FBS          FBC          CC      FIRG
 84.87        27.347        .54    53.807

MIDDLE CLOUD
    TG            TC          TT       TAUG       TAUC
291.34        260.91      214.5     1.8136     .60971
FIP = .49661
FIP = .18684
FIP = -.79221
FIP = .63132
FIP = -.77721
FIP = -.26137
TBS             TBC
.65968        .83396
IROUT CLEAR = 269.44 IROUT CLOUD = 219.12
IROUT TOTAL = 242.26
EBS             EBC
.20779    9.85295E-2
   FBS          FBC          CC      FIRG
 84.87        40.243        .54    60.771

HIGH CLOUD
    TG            TC          TT       TAUG       TAUC
291.34         214.5      214.5     1.8136     .21765
FIP = .49661
FIP = 5.74964E-2
FIP = -.79221
FIP = .53169
FIP = -.78953
FIP = -5.74989E-2
TBS             TBC
.65968        5.9506
IROUT CLEAR = 269.44 IROUT CLOUD = 214.28
IROUT TOTAL = 239.65
EBS             EBC
.20779        .18839
   FBS          FBC          CC      FIRG
 84.87        76.943        .54    80.589
K  SUM1         SUM2          DT        TG          ER
3  227.89     246.93     -3.0464    288.29    .083592
NET IR OUT = 246.93 NET SOL IN = 227.89
NET SOLG DOWN = 162.21 NET IRG UP = 65.934
GROUND EMISSION = 391.62

ITERATION = 4
TG = 288.29 BETA = 2.8674
```

```
LOW CLOUD
    TG             TC         TT       TAUG       TAUC
288.29         273.63     212.26     1.8388     1.1571
FIP = .47081
FIP = .33091
FIP = -.78895
FIP = .63497
FIP = -.67549
FIP = -.50755
TBS               TBC
.62983         .72215
IROUT CLEAR = 246.65 IROUT CLOUD = 229.51
IROUT TOTAL = 237.4
EBS               EBC
.21105         .07130
   FBS            FBC         CC       FIRG
82.652         27.924        .54     53.099

MIDDLE CLOUD
    TG             TC         TT       TAUG       TAUC
288.29         258.18     212.26     1.8388     .72599
FIP = .47081
FIP = .20782
FIP = -.78895
FIP = .623
FIP = -.76948
FIP = -.2958
TBS               TBC
.62983          .8069
IROUT CLEAR = 246.65 IROUT CLOUD = 203.28
IROUT TOTAL = 223.23
EBS               EBC
.21105          .1037
   FBS            FBC         CC       FIRG
82.652         40.612        .54      59.95

HIGH CLOUD
    TG             TC         TT       TAUG       TAUC
288.29         212.26     212.26     1.8388     .25155
FIP = .47081
FIP = 6.53759E-2
FIP = -.78895
FIP = .51021
FIP = -.78611
FIP = -6.53858E-2
TBS               TBC
.62983         5.7089
IROUT CLEAR = 246.65 IROUT CLOUD = 197.11
IROUT TOTAL = 219.9
EBS               EBC
.21105         .19133
   FBS            FBC         CC       FIRG
82.652          74.93        .54     78.482
K  SUM1          SUM2         DT         TG         ER
4  227.89      226.78     .16713     288.46    .004852
NET IR OUT = 226.78 NET SOL IN = 227.89
```

```
NET SOLG DOWN = 162.21 NET IRG UP = 64.663
GROUND EMISSION = 392.53

ITERATION = 5
TG = 288.46 BETA = 2.9092

LOW CLOUD
   TG            TC          TT        TAUG        TAUC
288.46        273.78      212.38     1.8374      1.1509
FIP = .47227
FIP = .33079
FIP = -.78916
FIP = .63595
FIP = -.67658
FIP = -.50624
TBS             TBC
 .6315         .72397
IROUT CLEAR = 247.88 IROUT CLOUD = 230.62
IROUT TOTAL = 238.56
EBS             EBC
.21084         .07106
   FBS            FBC          CC        FIRG
82.762         27.893         .54     53.133

MIDDLE CLOUD
   TG            TC          TT        TAUG        TAUC
288.46        258.33      212.38     1.8374      .71933
FIP = .47227
FIP = .20677
FIP = -.78916
FIP = .62348
FIP = -.76997
FIP = -.29396
TBS             TBC
 .6315          .8085
IROUT CLEAR = 247.88 IROUT CLOUD = 204.15
IROUT TOTAL = 224.27
EBS             EBC
.21084          .1034
   FBS            FBC          CC        FIRG
82.762         40.588         .54     59.988

HIGH CLOUD
   TG            TC          TT        TAUG        TAUC
288.46        212.38      212.38     1.8374      .24924
FIP = .47227
FIP = 6.48471E-2
FIP = -.78916
FIP = .51138
FIP = -.78633
FIP = -6.48564E-2
TBS             TBC
 .6315         5.7227
IROUT CLEAR = 247.88 IROUT CLOUD = 198.04
IROUT TOTAL = 220.97
EBS             EBC
.21084         .19115
```

FBS	FBC	CC	FIRG	
82.762	75.032	.54	78.588	

K SUM1	SUM2	DT	TG	ER
5 227.89	227.87	.002	288.46	.000047

NET IR OUT = 227.87 NET SOL IN = 227.89
NET SOLG DOWN = 162.21 NET IRG UP = 64.725
GROUND EMISSION = 392.54
ITF=1: SURFACE TEMPERATURE COMPUTED

VERTICAL STRUCTURE

Z	P	T	TAP	TACB	TAC	TAUD
0.0	1000.00	288.46	.0000	1.7803	1.7916	1.8374
.1	990.00	287.90	.3631	1.7477	1.7591	1.8051
.2	980.00	287.35	.4979	1.7154	1.7270	1.7731
.3	970.00	286.79	.5989	1.6835	1.6952	1.7414
.3	960.00	286.22	.6823	1.6519	1.6637	1.7100
.4	950.00	285.65	.7541	1.6206	1.6325	1.6790
.5	940.00	285.08	.8177	1.5896	1.6016	1.6483
.6	930.00	284.50	.8749	1.5590	1.5711	1.6179
.7	920.00	283.92	.9270	1.5286	1.5409	1.5879
.8	910.00	283.33	.9748	1.4986	1.5110	1.5581
.9	900.00	282.73	1.0190	1.4689	1.4814	1.5287
1.0	890.00	282.13	1.0601	1.4395	1.4522	1.4997
1.1	880.00	281.53	1.0984	1.4104	1.4233	1.4709
1.2	870.00	280.91	1.1344	1.3816	1.3946	1.4425
1.3	860.00	280.30	1.1681	1.3532	1.3663	1.4143
1.4	850.00	279.67	1.1999	1.3250	1.3384	1.3865
1.4	840.00	279.05	1.2298	1.2972	1.3107	1.3591
1.5	830.00	278.41	1.2582	1.2697	1.2834	1.3319
1.6	820.00	277.77	1.2850	1.2424	1.2563	1.3051
1.7	810.00	277.12	1.3104	1.2155	1.2296	1.2786
1.8	800.00	276.47	1.3345	1.1889	1.2032	1.2524
1.9	790.00	275.81	1.3574	1.1626	1.1771	1.2265
2.0	780.00	275.14	1.3792	1.1367	1.1513	1.2010
2.2	770.00	274.47	1.3999	1.1110	1.1259	1.1758
2.3	760.00	273.78	1.4196	1.0856	1.1007	1.1509
2.4	750.00	273.09	1.4383	1.0605	1.0759	1.1263
2.5	740.00	272.40	1.4562	1.0358	1.0514	1.1020
2.6	730.00	271.69	1.4732	1.0113	1.0272	1.0781
2.7	720.00	270.98	1.4895	.9871	1.0033	1.0544
2.8	710.00	270.26	1.5049	.9633	.9797	1.0311
2.9	700.00	269.53	1.5197	.9397	.9564	1.0081
3.0	690.00	268.80	1.5338	.9164	.9334	.9854
3.1	680.00	268.05	1.5472	.8934	.9107	.9631
3.3	670.00	267.30	1.5600	.8708	.8884	.9410
3.4	660.00	266.53	1.5722	.8484	.8663	.9193
3.5	650.00	265.76	1.5839	.8262	.8446	.8979
3.6	640.00	264.98	1.5950	.8044	.8231	.8768
3.7	630.00	264.19	1.6056	.7829	.8020	.8560
3.9	620.00	263.38	1.6157	.7616	.7811	.8355
4.0	610.00	262.57	1.6253	.7407	.7605	.8154
4.1	600.00	261.75	1.6345	.7199	.7403	.7956
4.2	590.00	260.91	1.6433	.6995	.7203	.7760
4.4	580.00	260.06	1.6516	.6794	.7007	.7568
4.5	570.00	259.20	1.6595	.6595	.6813	.7379

4.6	560.00	258.33	1.6671	.6398	.6622	.7193
4.8	550.00	257.45	1.6743	.6205	.6434	.7011
4.9	540.00	256.55	1.6812	.6013	.6249	.6831
5.0	530.00	255.64	1.6878	.5825	.6067	.6654
5.2	520.00	254.72	1.6940	.5638	.5888	.6481
5.3	510.00	253.78	1.6999	.5454	.5711	.6310
5.5	500.00	252.82	1.7055	.5273	.5537	.6143
5.6	490.00	251.85	1.7109	.5093	.5366	.5979
5.8	480.00	250.87	1.7160	.4916	.5198	.5818
5.9	470.00	249.87	1.7208	.4741	.5032	.5659
6.1	460.00	248.85	1.7254	.4567	.4869	.5504
6.3	450.00	247.81	1.7298	.4395	.4708	.5352
6.4	440.00	246.75	1.7340	.4225	.4550	.5203
6.6	430.00	245.67	1.7379	.4057	.4394	.5057
6.8	420.00	244.58	1.7417	.3889	.4241	.4914
6.9	410.00	243.46	1.7452	.3722	.4090	.4774
7.1	400.00	242.32	1.7486	.3556	.3942	.4637
7.3	390.00	241.15	1.7518	.3391	.3795	.4503
7.5	380.00	239.96	1.7549	.3225	.3650	.4372
7.6	370.00	238.75	1.7578	.3058	.3508	.4244
7.8	360.00	237.51	1.7605	.2890	.3367	.4119
8.0	350.00	236.24	1.7632	.2720	.3228	.3996
8.2	340.00	234.94	1.7657	.2546	.3090	.3877
8.4	330.00	233.61	1.7680	.2366	.2953	.3760
8.6	320.00	232.25	1.7703	.2178	.2817	.3646
8.9	310.00	230.85	1.7725	.1978	.2681	.3535
9.1	300.00	229.41	1.7745	.1758	.2545	.3427
9.3	290.00	227.94	1.7765	.1504	.2409	.3322
9.5	280.00	226.42	1.7784	.1174	.2272	.3219
9.8	270.00	224.86	1.7803	.0000	.2132	.3120
10.0	260.00	223.25	1.7820	.1152	.1988	.3022
10.3	250.00	221.59	1.7837	.1442	.1837	.2928
10.6	240.00	219.88	1.7854	.1643	.1678	.2836
10.8	230.00	218.11	1.7870	.1800	.1502	.2746
11.1	220.00	216.27	1.7885	.1929	.1299	.2659
11.4	210.00	214.36	1.7901	.2038	.1032	.2575
11.7	200.00	212.38	1.7916	.2132	.0000	.2492
12.0	190.00	212.38	1.7930	.2214	.1014	.2412
12.4	180.00	212.38	1.7945	.2286	.1248	.2335
12.7	170.00	212.38	1.7960	.2351	.1408	.2259
13.1	160.00	212.38	1.7975	.2410	.1532	.2185
13.5	150.00	212.38	1.7990	.2464	.1634	.2113
13.9	140.00	212.38	1.8006	.2513	.1720	.2042
14.4	130.00	212.38	1.8022	.2559	.1795	.1972
14.9	120.00	212.38	1.8038	.2602	.1862	.1904
15.4	110.00	212.38	1.8055	.2642	.1922	.1836
16.0	100.00	212.38	1.8074	.2682	.1977	.1768
16.7	90.00	212.38	1.8093	.2720	.2029	.1700
17.4	80.00	212.38	1.8114	.2758	.2079	.1630
18.2	70.00	212.38	1.8137	.2797	.2127	.1558
19.2	60.00	212.38	1.8162	.2836	.2175	.1481
20.3	50.00	212.38	1.8189	.2878	.2224	.1399
21.7	40.00	212.38	1.8220	.2921	.2274	.1306
23.5	30.00	212.38	1.8254	.2968	.2326	.1196
26.0	20.00	212.38	1.8293	.3018	.2381	.1059
30.3	10.00	212.38	1.8335	.3071	.2439	.0863
100.	0.00	212.38	1.8374	.3120	.2492	0.0000

Input for a 3 cloud model, with ITF = 0
Local conditions
Filename = SRCINB

```
So   =    1367.0
Mu   =       0.5
Day  =       0.5
Rg   =      0.13
Eg   =      1.00
Pg   =     1000.
Gam  =       6.5
Pt   =      200.
Ac   =      0.54
CO2  =      0.54
H2O  =      2.17
O3   =       .31
CH4  =     .0009
rh0  =      0.77
Pcl  =      0.76
Pcm  =      0.56
Pch  =      0.20
Dpc  =      100.
Dpcm =       50.
Dpch =       70.
Tcl  =      20.0
Tcm  =      15.0
Tch  =       2.0
Tal  =        0.
Tam  =        0.
Tah  =        0.
Ecl  =       1.0
Ecm  =       1.0
Ech  =       0.3
Frl  =      0.34
Frm  =      0.28
Frh  =      0.38
To   =     288.5
ITF  =         0
```

Output for a 3 cloud model, with ITF = 0
Local conditions
Filename = SRCOUTB

SIMPLE CLIMATE MODEL

S0	AMU	DAY	RG	FLUX	CC	WH2O	WCO2	WO3	WCH4	LAP	PT	EG	RHO
1367.	.50	.50	.13	341.75	.54	2.17	.54	.31	.00090	6.5	200.	1.00	.77

CLOUD PROPERTIES

	LOW	MIDDLE	HIGH
PC	.76	.56	.20
DPC	100.	50.0	70.0
CLT	20.0	15.0	2.0
CLA	0.0	0.0	0.0
EC	1.00	1.00	.30
FR	.34	.28	.38

```
ITERATION = 1
TG = 288.5 BETA = 2.9203

LOW CLOUD

   TG              TC          TT       TAUG       TAUC
288.5          273.83      212.42      1.837     1.1492
FIP = .47265
FIP = .33076
FIP = -.78921
FIP = .6362
FIP = -.67687
FIP = -.50589
  TBS             TBC
.63195         .72445
IROUT CLEAR = 248.21 IROUT CLOUD = 230.92
IROUT TOTAL = 238.87
  EBS             EBC
.21079         .07100
  FBS             FBC          CC       FIRG
82.792         27.885         .54     53.142

MIDDLE CLOUD
   TG              TC          TT       TAUG       TAUC
288.5          258.37      212.42      1.837     .71758
FIP = .47265
FIP = .20649
FIP = -.78921
FIP = .6236
FIP = -.77009
FIP = -.29348
  TBS             TBC
.63195         .80892
IROUT CLEAR = 248.21 IROUT CLOUD = 204.38
IROUT TOTAL = 224.54
  EBS             EBC
.21079         .10332
  FBS             FBC          CC       FIRG
82.792         40.582         .54     59.998

HIGH CLOUD
   TG              TC          TT       TAUG       TAUC
```

```
288.5          212.42     212.42      1.837     .24864
FIP = .47265
FIP = 6.47093E-2
FIP = -.78921
FIP = .51168
FIP = -.78639
FIP = -6.47185E-2
  TBS             TBC
.63195         5.7263
IROUT CLEAR = 248.21 IROUT CLOUD = 198.29
IROUT TOTAL = 221.25
  EBS             EBC
.21079          .1911
  FBS             FBC         CC        FIRG
82.792         75.059        .54     78.616
    K            SUM1       SUM2          DT          TG          ER
    1          227.89     228.16      -288.5       288.5     .001226
NET IR OUT = 228.16 NET SOL IN = 227.89
NET SOLG DOWN = 162.21 NET IRG UP = 64.742
GROUND EMISSION = 392.77
ITF=0: SURFACE TEMPERATURE SPECIFIED
```

VERTICAL STRUCTURE

Z	P	T	TAP	TACB	TAC	TAUD
0.0	1000.00	288.50	0.000	1.7800	1.7912	1.8370
.1	990.00	287.95	.3635	1.7473	1.7587	1.8046
.2	980.00	287.39	.4984	1.7150	1.7265	1.7725
.3	970.00	286.83	.5995	1.6830	1.6946	1.7408
.3	960.00	286.27	.6829	1.6513	1.6630	1.7094
.4	950.00	285.70	.7548	1.6199	1.6318	1.6783
.5	940.00	285.12	.8185	1.5889	1.6009	1.6475
.6	930.00	284.54	.8757	1.5582	1.5703	1.6170
.7	920.00	283.96	.9278	1.5278	1.5400	1.5869
.8	910.00	283.37	.9756	1.4977	1.5100	1.5571
.9	900.00	282.78	1.0199	1.4679	1.4804	1.5277
1.0	890.00	282.18	1.0610	1.4385	1.4511	1.4985
1.1	880.00	281.57	1.0993	1.4093	1.4221	1.4697
1.2	870.00	280.96	1.1352	1.3805	1.3935	1.4412
1.3	860.00	280.34	1.1690	1.3520	1.3651	1.4131
1.4	850.00	279.72	1.2007	1.3238	1.3371	1.3852
1.4	840.00	279.09	1.2307	1.2959	1.3094	1.3577
1.5	830.00	278.45	1.2590	1.2683	1.2820	1.3305
1.6	820.00	277.81	1.2858	1.2411	1.2549	1.3036
1.7	810.00	277.16	1.3112	1.2142	1.2282	1.2771
1.8	800.00	276.51	1.3353	1.1875	1.2017	1.2509
1.9	790.00	275.85	1.3582	1.1612	1.1756	1.2250
2.0	780.00	275.18	1.3800	1.1352	1.1498	1.1994
2.2	770.00	274.51	1.4007	1.1095	1.1243	1.1741
2.3	760.00	273.83	1.4203	1.0841	1.0991	1.1492
2.4	750.00	273.14	1.4391	1.0590	1.0743	1.1246
2.5	740.00	272.44	1.4569	1.0342	1.0497	1.1003
2.6	730.00	271.74	1.4739	1.0097	1.0255	1.0763
2.7	720.00	271.02	1.4901	.9855	1.0016	1.0527

2.8	710.00	270.30	1.5056	.9617	.9780	1.0294
2.9	700.00	269.58	1.5203	.9381	.9547	1.0064
3.0	690.00	268.84	1.5344	.9148	.9317	.9837
3.1	680.00	268.09	1.5478	.8918	.9090	.9613
3.3	670.00	267.34	1.5605	.8691	.8866	.9392
3.4	660.00	266.58	1.5727	.8467	.8646	.9175
3.5	650.00	265.80	1.5843	.8246	.8428	.8961
3.6	640.00	265.02	1.5954	.8028	.8214	.8750
3.7	630.00	264.23	1.6060	.7812	.8002	.8542
3.9	620.00	263.42	1.6161	.7600	.7794	.8337
4.0	610.00	262.61	1.6257	.7390	.7588	.8136
4.1	600.00	261.79	1.6348	.7183	.7386	.7938
4.2	590.00	260.95	1.6436	.6979	.7186	.7742
4.4	580.00	260.10	1.6519	.6778	.6990	.7550
4.5	570.00	259.24	1.6598	.6579	.6796	.7362
4.6	560.00	258.37	1.6674	.6383	.6605	.7176
4.8	550.00	257.49	1.6746	.6189	.6418	.6993
4.9	540.00	256.59	1.6814	.5998	.6233	.6814
5.0	530.00	255.68	1.6879	.5810	.6051	.6637
5.2	520.00	254.76	1.6941	.5624	.5871	.6464
5.3	510.00	253.82	1.7000	.5440	.5695	.6294
5.5	500.00	252.86	1.7056	.5258	.5521	.6127
5.6	490.00	251.89	1.7110	.5079	.5351	.5962
5.8	480.00	250.91	1.7160	.4902	.5182	.5802
5.9	470.00	249.90	1.7209	.4727	.5017	.5644
6.1	460.00	248.88	1.7254	.4554	.4854	.5489
6.3	450.00	247.85	1.7298	.4383	.4694	.5337
6.4	440.00	246.79	1.7339	.4213	.4536	.5188
6.6	430.00	245.71	1.7379	.4045	.4381	.5043
6.8	420.00	244.61	1.7416	.3877	.4228	.4900
6.9	410.00	243.49	1.7451	.3711	.4077	.4760
7.1	400.00	242.35	1.7485	.3546	.3929	.4623
7.3	390.00	241.19	1.7517	.3380	.3783	.4490
7.5	380.00	240.00	1.7547	.3215	.3639	.4359
7.6	370.00	238.79	1.7576	.3049	.3496	.4231
7.8	360.00	237.55	1.7604	.2881	.3356	.4106
8.0	350.00	236.28	1.7630	.2712	.3217	.3984
8.2	340.00	234.98	1.7655	.2538	.3080	.3865
8.4	330.00	233.65	1.7678	.2359	.2943	.3749
8.6	320.00	232.28	1.7701	.2172	.2808	.3636
8.9	310.00	230.88	1.7722	.1972	.2672	.3525
9.1	300.00	229.45	1.7743	.1753	.2537	.3417
9.3	290.00	227.97	1.7763	.1500	.2402	.3312
9.5	280.00	226.46	1.7782	.1171	.2265	.3210
9.8	270.00	224.90	1.7800	.0000	.2125	.3111
10.0	260.00	223.29	1.7817	.1149	.1982	.3014
10.3	250.00	221.63	1.7834	.1438	.1832	.2920
10.6	240.00	219.91	1.7851	.1639	.1673	.2828
10.8	230.00	218.14	1.7867	.1795	.1498	.2739
11.1	220.00	216.30	1.7882	.1923	.1296	.2652
11.4	210.00	214.40	1.7897	.2032	.1030	.2568
11.7	200.00	212.42	1.7912	.2125	.0000	.2486
12.0	190.00	212.42	1.7927	.2207	.1012	.2407
12.4	180.00	212.42	1.7942	.2279	.1245	.2329
12.7	170.00	212.42	1.7957	.2344	.1404	.2254
13.1	160.00	212.42	1.7972	.2402	.1528	.2180
13.5	150.00	212.42	1.7987	.2456	.1629	.2108

13.9	140.00	212.42	1.8002	.2505	.1715	.2038
14.4	130.00	212.42	1.8018	.2550	.1790	.1969
14.9	120.00	212.42	1.8035	.2593	.1857	.1901
15.4	110.00	212.42	1.8052	.2634	.1917	.1833
16.0	100.00	212.42	1.8070	.2673	.1972	.1766
16.7	90.00	212.42	1.8090	.2712	.2024	.1698
17.4	80.00	212.42	1.8111	.2750	.2073	.1628
18.2	70.00	212.42	1.8133	.2788	.2121	.1556
19.2	60.00	212.42	1.8158	.2828	.2169	.1480
20.3	50.00	212.42	1.8186	.2869	.2218	.1398
21.7	40.00	212.42	1.8216	.2912	.2268	.1305
23.5	30.00	212.42	1.8251	.2959	.2320	.1196
26.0	20.00	212.42	1.8289	.3009	.2375	.1059
30.3	10.00	212.42	1.8331	.3062	.2433	.0863
100.	0.00	212.42	1.8370	.3111	.2486	0.0000

ACKNOWLEDGMENTS

It is a pleasure to thank Liz Gyurasits for her valuable editorial effort, and Glen Riley, Arthur Johnston and Robert Fry for for their helpful comments.

REFERENCES

Beard, J.T. & Hollen, D.K. (1969). The influence of solar radiation reflectance on water evaporation. WRRC Bull. 30, Virginia Polytechnic Institute, Blacksburg, VA, 26 pp.

Climatic Change (1983). Report of the Carbon Dioxide Assessment Committee. National Academy Press, Washington, DC, 496 pp.

Frohlich, C. (1983). Data on total and spectral solar irradiance. *Comments Appl. Opt.* **22**, 3928.

Green, A.E.S. (1964). Attenuation by ozone and the earth's albedo in the middle ultraviolet. *Appl. Opt.* **3**, 203-208.

Hansen, J.E., Russell, G., Lacis, A.A., Fung, I., Ring, D. & Stone, P. (1985). Climate response times: Dependence on sensitivity and ocean mixing. *Science* **229**, 857-859.

Henderson-Sellers, A. & Wilson, M.F. (1983). Surface albedo data for climate modelling. *Rev. Geophys. Space. Phys.* **21**, 1743-1778.

Hobson, D.E. & Williams, D. (1971). Infrared spectral reflectance of sea water. *Appl. Opt.* **10**, 2372-2373.

Houghton, J.T. (1979). The physics of atmospheres. Cambridge University Press, Cambridge, 203 pp.

Huillet, T. & Lauga, J. (1985). A soil-plant-water model with a case study in a forested catchment. *Ecol. Modelling* **27**, 235-250.

Kontratyev, K.YA. (1969). Radiation in the atmosphere. Academic Press, New York, 907 pp.

Lacis, A.A. & Hansen, J.E. (1974). A parameterization for the absorption of solar radiation in the earth's atmosphere. *J. Atmos. Sci.* **31**, 118-133.

London, J. (1957). A study of the atmospheric heat balance, final report. Coll. Eng. Res. Div., New York University, New York, 99 pp.

Manabe, S. & Strickler, R.F. (1964). Thermal equilibrium of an atmosphere with a convective adjustment. *J. Atmos. Sci.* **21**, 261-385.

Peng, L.I., Chou, M.-D. & Arking, A. (1982). Climate studies with a multi-layer energy balance model. Part I: model description and sensitivity to the solar constant. *J. Atmos. Sci.* **39**, 2639-2656.

Sagan, C. & Pollack, J.B. (1967). Anisotropic non-conservative scattering and the clouds of Venus. *J. Geophys. Res.* **72**, 469-477.

Sasamori, T., London, J. & Hoyt, D.V. (1972). Radiation budget of the southern hemisphere. *Meterol. Mongr.* **13**, 9-23.

Stephens, G.L., Campbell, G.G. & Vonder Haar, T.H. (1981). Earth radiation budgets. *J. Geophys. Res.* **86**, 9739-9760.

U.S. Standard Atmosphere (1976). NOAA-S/T76-1562, U.S. Government Printing Office, Washington, DC, 227 pp.

Vardavas, I.M. (1987*a*). Atmospheric temperature response to solar cycle uv flux variations. *Solar Physics* **108**, 403-410.

Vardavas, I.M. (1987*b*). Modelling the seasonal variation of net all-wave radiation flux and evaporation in a tropical wet-dry region. *Ecological Modelling* **39**, 247-268.

Vardavas, I.M. & Carver, J.H. (1984*a*). Comments on the Newton-Raphson method for obtaining temperature profiles from radiative-convective models. *Planet. Space Sci.* **32**, 803-807.

Vardavas, I.M. & Carver, J.H., (1984*b*). Solar and terrestrial parameterization for radiative-convective models. *Planet. Space Sci.* **32**, 1307-1325.

Vardavas, I.M. & Carver, J.H. (1985). Atmospheric temperature response to variations in CO_2 concentration and the solar-constant. *Planet. Space Sci.* **33**, 1187-1207.

Yamamoto, G. (1962). Direct absorption of solar radiation by atmospheric water vapour, carbon dioxide and molecular oxygen. *J. Atmos. Sci.* **19**, 182-188.

SUPERVISING SCIENTIST FOR THE ALLIGATOR RIVERS REGION

RESEARCH PUBLICATIONS

Alligator Rivers Region Research Institute Research Report 1983-84
Alligator Rivers Region Research Institute Annual Research Summary 1984-85
Alligator Rivers Region Research Institute Annual Research Summary 1985-86
Alligator Rivers Region Research Institute Annual Research Summary 1986-87
Alligator Rivers Region Research Institute Annual Research Summary 1987-88

Research Reports (RR) and Technical Memoranda (TM)

RR 1	The macroinvertebrates of Magela Creek, Northern Territory. April 1982 (pb, mf - 46 pp.)	R. Marchant
RR 2	Water quality characteristics of eight billabongs in the Magela Creek catchment. December 1982 (pb, mf - 60 pp.)	B.T. Hart & R.J. McGregor
RR 3	A limnological survey of the Alligator Rivers Region. I. Diatoms (Bacillariophyceae) of the Region. August 1983 (pb, mf - 160 pp.)	D.P. Thomas
	*A limnological survey of the Alligator Rivers Region. II. Freshwater algae, exclusive of diatoms. 1986 (pb, mf - 176 pp.)	H.U. Ling & P.A. Tyler
RR 4	*Ecological studies on the freshwater fishes of the Alligator Rivers Region, Northern Territory. Volume I. Outline of the study, summary, conclusions and recommendations. 1986 (pb, mf - 63 pp.)	K.A. Bishop, S.A. Allen, D.A. Pollard & M.G. Cook
	Ecological studies on the freshwater fishes of the Alligator Rivers Region, Northern Territory. Volume II. (in press)	K.A. Bishop, S.A. Allen, D.A. Pollard & M.G. Cook
	Ecological studies on the freshwater fishes of the Alligator Rivers Region, Northern Territory. Volume III. (in press)	K.A. Bishop, S.A. Allen, D.A. Pollard & M.G. Cook
RR 5	Macrophyte vegetation of the Magela Creek flood plain, Alligator Rivers Region, Northern Territory. March 1989 (pb - 41 pp.)	C.M. Finlayson, B.J. Bailey & I.D. Cowie
TM 1	Transport of trace metals in the Magela Creek system, Northern Territory. I. Concentrations and loads of iron, manganese, cadmium, copper, lead and zinc during flood periods in the 1978-1979 Wet season. December 1981 (pb, mf - 27 pp.)	B.T. Hart, S.H.R. Davies & P.A. Thomas
TM 2	Transport of trace metals in the Magela Creek system, Northern Territory. II. Trace metals in the Magela Creek billabongs at the end of the 1978 Dry season. December 1981 (pb, mf - 23 pp.)	S.H.R. Davies & B.T. Hart
TM 3	Transport of trace metals in the Magela Creek system, Northern Territory. III. Billabong sediments. December 1981 (pb, mf - 24 pp.)	P.A. Thomas, S.H.R. Davies & B.T. Hart
TM 4	The foraging behaviour of herons and egrets on the Magela Creek flood plain, Northern Territory. March 1982 (pb, mf - 20 pp.)	H.R. Recher & R.T. Holmes
TM 5	Flocculation of retention pond water. May 1982 (pb, mf - 8 pp.)	B.T. Hart & R.J. McGregor
TM 6	Dietary pathways through lizards of the Alligator Rivers Region Northern Territory. July 1984 (pb, mf - 15 pp.)	C.D. James, S.R. Morton, R.W. Braithwaite & J.C. Wombey
TM 7	Capacity of waters in the Magela Creek system, Northern Territory, to complex copper and cadmium. August 1984 (pb, mf - 42 pp.)	B.T. Hart & S.H.R. Davies
TM 8	Acute toxicity of copper and zinc to three fish species from the Alligator Rivers Region. August 1984 (pb, mf - 31 pp.)	L. Baker & D. Walden

* available from AGPS, Canberra
pb = available as paperback; mf = available as microfiche

TM 9	Textural characteristics and heavy metal concentrations in billabong sediments from the Magela Creek system, northern Australia. October 1984 (pb, mf - 39 pp.)	P.A. Thomas & B.T. Hart
TM 10	Oxidation of manganese(II) in Island Billabong water. October 1984 (pb, mf - 11 pp.)	B.T. Hart & M.J. Jones
TM 11	*In situ* experiments to determine the uptake of copper by the aquatic macrophyte *Najas tenuifolia* R.Br. December 1984 (pb, mf - 13 pp.)	B.T. Hart, M.J. Jones & P. Breen
TM 12	Use of plastic enclosures in determining the effects of heavy metals added to Gulungul Billabong. January 1985 (pb, mf - 25 pp.)	B.T. Hart, M.J. Jones & P. Bek
TM 13	Fate, of heavy metals in the Magela Creek system, northern Australia. I. Experiments with plastic enclosures placed in Island Billabong during the 1980 Dry Season: heavy metals. May 1985 (pb, mf - 46 pp.)	B.T. Hart, M.J. Jones & P. Bek
TM 14	Fate of heavy metals in the Magela Creek system, northern Australia. II. Experiments with plastic enclosures placed in Island Billabong during the 1980 Dry season: limnology and phytoplankton. May 1985 (pb, mf - 32 pp.)	B.T. Hart, M.J. Jones, P. Bek & J. Kessell
TM 15	Use of fluorometric dye tracing to simulate dispersion of discharge from a mine site. A study of the Magela Creek system, March 1978. January 1986 (pb, mf - 51 pp.)	D.I. Smith, P.C. Young & R.J. Goldberg
TM 16	Diets and abundances of aquatic and semi-aquatic reptiles in the Alligator Rivers Region. July 1986 (pb, mf - 57 pp.)	R. Shine
TM 17	Plants of the Alligator Rivers Region, Northern Territory. August 1986 (pb, mf - 54 pp.)	I.E. Cowie & C.M. Finlayson
TM 18	The taxonomy and seasonal population dynamics of some Magela Creek flood plain microcrustaceans (Cladocera and Copepoda) September 1986 (pb, mf - 80 pp.)	M.E. Julli
TM 19	Frogs of the Magela Creek system. January 1987 (pb, mf - 46 pp.)	M.J. Tyler & G.A. Crook
TM 20	Radiation exposure of members of the public resulting from operation of the Ranger Uranium Mine. December 1987 (pb, mf - 22 pp.)	A. Johnston
TM 21	Interlaboratory comparison of the measurement of uranium in urine. June 1988 (pb - 24 pp.)	T. Anttonen, B.N. Noller & D.A. Woods
TM 22	Biology and early development of eight fish species from the Alligator Rivers Region. June 1988 (pb - 68 pp.)	W. Ivantsoff, L.E.L.M. Crowley, E. Howe & G. Semple
TM 23	Alien plants in the Alligator Rivers Region, Northern Territory, Australia. September 1988 (pb - 34 pp.)	I.D. Cowie, C.M. Finlayson & B.J. Bailey
TM 24	The determination of zinc in Magela Creek water April 1989 (pb - 26 pp.)	C.A.A. LeGras & B.N. Noller
TM 25	Element concentrations in the freshwater mussel, *Velesunio angasi*, in the Alligator Rivers Region June 1989 (pb - 262 pp.	H.E. Allison & R.D. Simpson

* available from AGPS, Canberra
pb = available as paperback; mf = available as microfiche